AGU PUBLICATIONS

JGR

Journal of Geophysical Research: Biogeosciences

RESEARCH ARTICLE

10.1002/2014JG002817

Key Points:

- Soil CO_2, CH_4, and N_2O emissions were independent of C inputs
- CO_2 and CH_4 fluxes varied along gradients in soil wetness and texture
- This floodplain is losing C likely due to long-term drying from urbanization

Correspondence to:
G. B. Noe,
gnoe@usgs.gov

Citation:
Batson, J., G. B. Noe, C. R. Hupp, K. W. Krauss, N. B. Rybicki, and E. R. Schenk (2015), Soil greenhouse gas emissions and carbon budgeting in a short-hydroperiod floodplain wetland, *J. Geophys. Res. Biogeosci.*, *120*, 77–95, doi:10.1002/2014JG002817.

Received 30 SEP 2014
Accepted 21 DEC 2014
Accepted article online 29 DEC 2014
Published online 21 JAN 2015

Soil greenhouse gas emissions and carbon budgeting in a short-hydroperiod floodplain wetland

Jackie Batson[1], Gregory B. Noe[1], Cliff R. Hupp[1], Ken W. Krauss[2], Nancy B. Rybicki[1], and Edward R. Schenk[1]

[1]National Research Program, U.S. Geological Survey, Reston, Virginia, USA, [2]National Wetlands Research Center, U.S. Geological Survey, Lafayette, Louisiana, USA

Abstract Understanding the controls on floodplain carbon (C) cycling is important for assessing greenhouse gas emissions and the potential for C sequestration in river-floodplain ecosystems. We hypothesized that greater hydrologic connectivity would increase C inputs to floodplains that would not only stimulate soil C gas emissions but also sequester more C in soils. In an urban Piedmont river (151 km^2 watershed) with a floodplain that is dry most of the year, we quantified soil CO_2, CH_4, and N_2O net emissions along gradients of floodplain hydrologic connectivity, identified controls on soil aerobic and anaerobic respiration, and developed a floodplain soil C budget. Sites were chosen along a longitudinal river gradient and across lateral floodplain geomorphic units (levee, backswamp, and toe slope). CO_2 emissions decreased downstream in backswamps and toe slopes and were high on the levees. CH_4 and N_2O fluxes were near zero; however, CH_4 emissions were highest in the backswamp. Annual CO_2 emissions correlated negatively with soil water-filled pore space and positively with variables related to drier, coarser soil. Conversely, annual CH_4 emissions had the opposite pattern of CO_2. Spatial variation in aerobic and anaerobic respiration was thus controlled by oxygen availability but was not related to C inputs from sedimentation or vegetation. The annual mean soil CO_2 emission rate was 1091 g C m^{-2} yr^{-1}, the net sedimentation rate was 111 g C m^{-2} yr^{-1}, and the vegetation production rate was 240 g C m^{-2} yr^{-1}, with a soil C balance (loss) of −338 g C m^{-2} yr^{-1}. This floodplain is losing C likely due to long-term drying from watershed urbanization.

1. Introduction

The global terrestrial carbon (C) budget demonstrates that more C is stored in soil (1672 Pg) than in the atmosphere (738 Pg) and plant biomass (850 Pg) combined [*Reddy and DeLaune*, 2008]. While constituting only 5–8% of the terrestrial land surface, wetlands store 535 Pg or approximately 30% of global soil C, making wetlands a major portion of the terrestrial C budget [*Whiting and Chanton*, 1993; *Bridgham et al.*, 2006; *Mitsch and Gosselink*, 2007]. Carbon accumulates in wetlands due to root volume expansion and canopy litter/wood contributions to the soil, as well as slow decomposition of organic matter in flooded soils where reducing soil conditions suppress efficient aerobic respiration and CO_2 production. However, anaerobic methanogenesis may increase emissions of CH_4, a potent greenhouse gas (GHG) with 25 times the global warming potential of CO_2 [*Forster et al.*, 2007]. This could offset the climate effects of sequestering atmospheric C in soil [*Bridgham et al.*, 2006]. Wetlands appear to be a small to moderate C sink but are believed to contribute 15–40% of global CH_4 [*Segers*, 1998]. An additional concern regarding wetland influence on global climate is emission of nitrous oxide (N_2O), another powerful GHG [*Verhoeven et al.*, 2006]. Thus, improved estimates of soil GHG emission rates, C sinks, and C sources from a range of wetland types is critical to better understand and predict global change.

Hydrologic and temperature controls on CO_2 and CH_4 fluxes in wetlands have been well documented [e.g., *Altor and Mitsch*, 2006, 2008; *Couwenberg et al.*, 2010; *Nahlik and Mitsch*, 2010; *Sha et al.*, 2011]. Aerobic respiration and anaerobic fermentation release CO_2 from the soil through oxidation of soil organic matter. Methane production often increases with water table elevation and the resulting lack of oxygen as a terminal electron acceptor for respiration. Decomposition rates increase exponentially with temperature due to increased microbial and plant activity, and decrease with soil saturation [*Megonigal and Schlesinger*, 1997]. The amount and quality of decomposable substrate also influences CH_4 emissions [*Segers*, 1998]; the addition

©2014. American Geophysical Union. All Rights Reserved.

of carbon to substrate-limited soils increases both aerobic and anaerobic respiration [e.g., *Bridgham and Richardson*, 1992].

Floodplains of streams and small rivers outside of lowlands are generally drier than other wetlands [*Hupp*, 2000], and the role of floodplain wetlands in C cycling and climate regulation is less understood than most wetland ecosystem types. However, floodplain wetlands are now understood to provide important ecosystem services such as flood mitigation, downstream water quality improvement, recreation, and wildlife habitat. Many floodplain ecosystems have been altered by anthropogenic changes to hydrology and geomorphology [*Tockner and Stanford*, 2002; *Groffman et al*., 2003; *Hupp et al*., 2009]; to understand the impacts of human hydrological modifications on floodplain ecology, we must first understand the processes driving floodplain function. Floodplain wetlands exist at the interface between terrestrial uplands and flowing streams, where hydrogeomorphic, vegetative, and nutrient biogeochemical processes interact and produce complex feedbacks that make them difficult to study [*Naiman and Décamps*, 1997; *Noe*, 2013]. However, these interactions provide "hot spots" and "hot moments" of biogeochemical activity [*McClain et al*., 2003] in floodplain wetlands.

Variation in hydrologic connectivity generates gradients in floodplain hydrogeomorphology and ecosystem functions. Floodplain processes are best understood in four dimensions: longitudinal, lateral, vertical, and temporal [*Amoros et al*., 1987; *Ward*, 1989; *Poole*, 2010; *Noe*, 2013]. Longitudinal gradients are expected in physical, biological, and chemical characteristics from headwaters to mouth of streams and floodplains [*Vannote et al*., 1980; *Hupp*, 1986; *Hupp et al*., 2013]. Lateral gradients in hydrogeomorphology have been shown to influence denitrification [*Richardson et al*., 2004; *Welti et al*., 2012], N and P mineralization rates [*Noe et al*., 2013], primary production [*Burke et al*., 1999], vegetative nutrient fluxes [*Clawson et al*., 2001], nutrient sedimentation [*Noe and Hupp*, 2005, 2009], and potential microbial respiration [*Welti et al*., 2012]. Pulses of flood water provide carbon and nutrient subsidies that, in part, control vegetation, animal communities, and biogeochemistry along gradients of hydrologic connectivity [*Junk et al*., 1989; *Bayley*, 1995]. The rapid exchange of energy and materials in these open-flow floodplain wetlands make them more productive [*Spink et al*., 1998; *Tockner and Stanford*, 2002] with faster biogeochemical cycling than hydrologically closed wetlands [*Hopkinson*, 1992; *Wolf et al*., 2013]. *Welti et al*. [2012] studied substrate-induced potential respiration along a hydrogeomorphic gradient, but the interactive effects of gradients in hydrology, soil characteristics, and sediment C and nutrient input fluxes on in situ floodplain soil respiration rates have not been observed.

Floodplains often trap large amounts of C through sedimentation [*Craft and Casey*, 2000; *Noe and Hupp*, 2005; *Hupp et al*., 2008; *Noe and Hupp*, 2009]. Particulate and dissolved organic C, both electron donors, are delivered to the floodplain primarily through allochthonous sediment-laden flood water and autochthonous vegetative production. The role of C sedimentation in C accumulation is not well understood in freshwater mineral soil wetlands (e.g., floodplains) but could be a meaningful flux at continental scales [*Bridgham et al*., 2006]. Deposited C can be preserved in deep soil layers by burial with sediment, and eroded floodplain sediment can eventually be buried in the ocean [*Zehetner et al*., 2009]. Both the loading of C to the floodplain and the export of C to downstream food webs are dependent upon the degree of floodplain hydrologic connectivity [*Battin et al*., 2008]; rivers thus play an important role in the global C cycle [*Battin et al*., 2009]. However, the fate of C deposited on floodplain soils is very uncertain. Carbon accumulation could be offset by CH_4 emissions during inundated reducing conditions and CO_2 emissions during dry oxidizing conditions. The combination of high inputs of C and frequently aerobic soils should stimulate C respiration in floodplain soils and influence the balance of C inputs and losses, with spatial variation across the hydrogeomorphic gradients of floodplains. Measurable long-term accumulation of C in floodplain soils [e.g., *Craft and Casey*, 2000] indicates that inputs can exceed outputs, including soil microbial respiration, but how widespread is net C accumulation in floodplain soils?

Here we quantified the fluxes of sediment and vegetation C inputs versus C outgassing from soils and C erosion from stream banks to help clarify whether floodplain wetlands are a net source or sink of carbon. The objectives of our study were to (1) quantify rates of aerobic and anaerobic soil C respiration and floodplain CO_2, CH_4, and N_2O emissions; (2) assess the effect of lateral and longitudinal gradients in hydrologic connectivity on floodplain soil respiration; (3) determine the environmental controls on soil respiration from a large suite of measured ecosystem variables in the Difficult Run floodplain; and (4) incorporate inputs of

©2014. American Geophysical Union. All Rights Reserved.

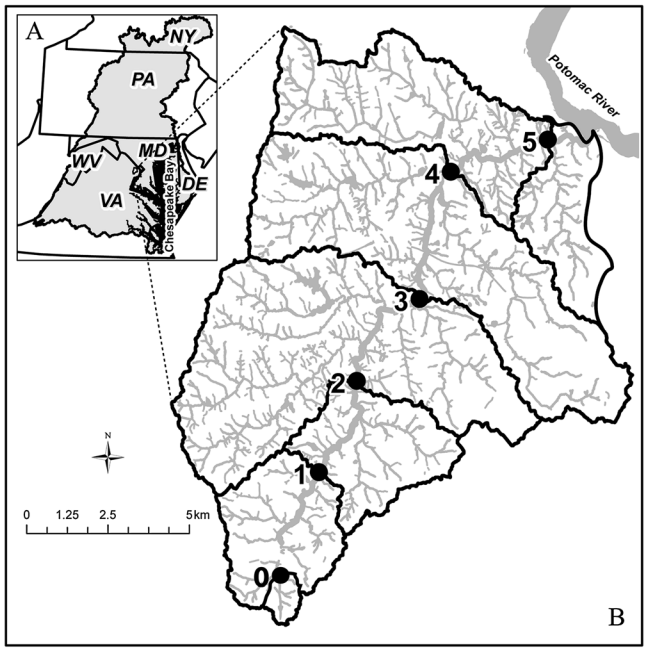

Figure 1. (a) Map showing location of Difficult Run study site within the Chesapeake Bay watershed. (b) Map of the Difficult Run watershed, showing sites 0–5 and their respective catchments.

C from litterfall and sedimentation and outputs from CO_2 and CH_4 emissions and bank erosion into a preliminary C budget for these wetlands. We hypothesized that CO_2 flux would be greatest in drier locations (higher elevation in the lateral direction and upstream sites in the longitudinal direction), and CH_4 fluxes would be greatest in wetter locations (lower elevations and downstream locations). We expected that soil C respiration would also correlate with other microbial processes that are influenced by hydrology and sediment inputs, such as N and P mineralization. We further hypothesized that floodplain locations with greater hydrologic connectivity to the river would have greater C inputs that would stimulate soil C gas emissions, but that inputs would exceed losses and result in the sequestration of more soil C. This study adds to our limited understanding of wetland carbon processing in multiple dimensions of hydrologic connectivity and further explains feedbacks between vegetation, hydrogeomorphology, and biogeochemistry.

2. Methods

2.1. Site Location and Sampling Design

Our 2 year study was conducted on the floodplain of Difficult Run, a fifth-order stream in the crystalline (gneiss and schist bedrock) Piedmont of Virginia, USA, that is tributary to the Potomac River and the Chesapeake Bay (Figure 1). Streams of this region are typically pool-riffle systems flowing over a gravel bed with considerable fine-grained deposits of legacy sediment on floodplains and terraces due to post-colonial upland erosion [*Hupp et al*., 2013]. Typical of the eastern U.S., the Difficult Run watershed saw extensive colonial land clearing and row-crop agriculture, followed by upland erosion and bottomland sediment deposition. Row-crop agriculture was followed by pasture and dairy farms until the midtwentieth century, when fields reverted to second-growth forest. The area rapidly began to urbanize in the mid-1960s through the 1990s, resulting in increased flood frequency [*Hupp et al*., 2013]. Today, land use in the Difficult Run watershed is mixed urban (58%, including suburban), forest (37%), agriculture (2%), and other land uses (5%). Mean annual discharge in the 151 km^2 watershed is 1.77 $m^3 s^{-1}$ (1935–2013) [*U.S. Geological Survey*, 2013]. Due to the substantial depths of legacy sediment and moderate watershed slope, Piedmont floodplains are relatively dry floodplains [*Hupp et al*., 2013; *Noe et al*., 2013].

Six floodplain study sites were selected along the longitudinal gradient from near the headwaters to near the mouth of Difficult Run. Sites were chosen to span the watershed, have typical geomorphology and vegetation, and be publicly owned and managed as forested parkland (Fairfax County Park Authority). The cumulative catchment areas for sites 0, 1, 2, 3, 4, and 5 are 3, 14, 28, 74, 117, and 141 km^2, respectively (Figure 1). Site 0 has minor alluvial conditions with little development of typical fluvial landforms, while sites 1 through 5 have well-developed fluvial landforms (e.g., floodplains and in-channel bars).

Within each site, floodplains consist of three dominant lateral geomorphic units: higher elevation natural levees adjacent to the channel, lower elevation backswamp, and higher elevation toe slope adjacent to the uplands. Site 4 lacks a toe slope. Measurements were made to encompass these longitudinal and lateral gradients of hydrologic connectivity. Each site had three transects spaced 50 m apart and oriented

©2014. American Geophysical Union. All Rights Reserved.

perpendicular to the channel, beginning on the levee and ending on the toe slope in the transition from floodplain to upland. Sampling plots were located every 10 to 25 m along each transect and classified into one of the three geomorphic units based on site hydrogeomorphic interpretation and relative elevations. In each site, two replicate plots in each geomorphic unit were randomly selected from among transects for more detailed measurements of soil respiration and associated ecosystem attributes ($n = 34$) [see *Noe et al.*, 2013]. Measurements in each plot occurred within 2 m of each other.

2.2. Soil Respiration and Associated Measurements

Aerobic soil respiration, the sum of autotrophic root respiration and heterotrophic microbial respiration, was measured as the total flux of CO_2 from the soil surface. Periodic measurements were made in situ from January 2011 through December 2012 using an infrared gas analyzer (model LI-COR 8100, LI-COR Environmental Inc., Lincoln, NE, USA). Opaque, white PVC pipe (20 cm diameter, 10 cm length) was inserted 5 cm into the soil at each plot (avoiding woody stems) as a permanent soil collar 1 month prior to the beginning of measurements. After initial removal of aboveground herbaceous vegetation in each collar, any vegetation was clipped after each measurement to minimize disturbance immediately prior to measurement of gas flux. The sample chamber was placed over the soil collar for a 3.5 min incubation, over which the rate of CO_2 emission was calculated from a best fit linear or exponential regression of CO_2 concentration with time. CO_2 fluxes on an areal basis were then calculated from the flux equation [*Healy et al.*, 1996]:

$$F_c = \frac{10VP_0\left(1 - \frac{W_0}{1000}\right)}{RS(T_0 + 273.15)}\frac{\mathrm{d}CO_2}{\mathrm{d}t} \tag{1}$$

where $F_c = CO_2$ flux (μmol CO_2 m^{-2} s^{-1}), V = total volume (cm^3), P_0 = initial pressure (kPa), W_0 = initial water vapor mole fraction (mmol mol^{-1}), R = gas constant (8.314 Pa m^3 K^{-1} mol^{-1}), S = total soil surface area (cm^2), T_0 = initial chamber temperature (°C), and $\frac{\mathrm{d}CO_2}{\mathrm{d}t}$ = rate of change in CO_2 (μmol mol^{-1} s^{-1} or ppm s^{-1}). For budgeting, moles of CO_2 were converted to grams C.

CO_2 fluxes in 2011 were measured every 3 weeks at each site and plot in random site order. In 2012, CO_2 and CH_4 emissions were measured quarterly to include anaerobic C respiration as well. Prior to the 2012 measurements, the 20 cm diameter collars originally installed were replaced with 30 cm length pipes at six of the wettest sites so that GHG fluxes could be measured with the LI-8100 chamber during periods of higher surface water. The 3.5 min incubations were similarly used to calculate CO_2 flux in 2012; they then were followed by 20 min chamber incubations for CH_4 (and N_2O) flux. A nylon syringe was used to extract 15 mL gas samples from the LI-8100's sampling port every 5 min during the 20 min incubation, beginning 30 s after chamber closure to allow for gas mixing. Extracted samples were immediately transferred to vacuumed 5 mL Wheaton glass vials topped with gray butyl stoppers and aluminum seals. Gas samples were stored in the dark at room temperature and analyzed for CH_4 and N_2O within 1 week on a gas chromatograph equipped with flame-ionization and electron capture detectors (model Varian CP-3800, Agilent Technologies, Santa Clara, CA, USA) that was calibrated using certified standards (Scott Specialty Gases Inc., Plumsteadville, PA, USA). Methane and N_2O fluxes were calculated similarly to CO_2 fluxes.

Associated measurements of potential ecosystem predictors of C and GHG dynamics were also made simultaneously at each plot during the sampling periods. Soil temperature was measured by the LI-8100 simultaneously during each incubation with a temperature probe inserted 4 cm into the ground near the soil collar. Immediately following the incubations, soil redox potential was measured using an ExStik redox probe (ExTech Instruments, Nashua, NH, USA) placed in the ground near the collar. A sample of the top 5 cm of soil was also collected at the time of GHG measurement. A soil subsample was dried at 60°C until constant mass to estimate soil water-filled pore space (WFPS) as volumetric moisture ÷ [1- (bulk density ÷ quartz parent material density)]. Soil bulk density was reported in *Noe et al.* [2013]. Another subsample was air dried and analyzed for pH using a 1:2 soil to deionized water slurry [*Robertson et al.*, 1999].

Since all gas sampling occurred during the daytime, we analyzed soil temperatures measured 2.5 cm below the soil surface every 30 min for a year in each plot during a previous study [*Noe et al.*, 2013]. Minimal differences were found between annual mean daytime and nighttime soil temperatures, so we did not correct for differences in day and night fluxes due to temperature when calculating annual fluxes.

©2014. American Geophysical Union. All Rights Reserved.

2.3. Ecosystem Attributes

The Difficult Run floodplain has been studied for many additional ecosystem characteristics and processes that vary along gradients of hydrologic connectivity and could influence C cycling, including hydrologic inputs, vegetative inputs, soil quality, and nutrient mineralization. Hydrologic connectivity was evaluated using plot mean water level and hydroperiod. A pressure transducer (HOBO water level logger; Onset Computer Corporation, Bourne, MA, USA) was placed in a screened PVC well located near the lowest elevation plot at each site. Water levels were measured every 15 min beginning in November 2008. Mean water elevation relative to soil surface and hydroperiod (percentage of observations with water elevation above soil surface) for each plot were calculated using the transducer water level readings and a laser level survey of each plot relative to the well. To further explore possible long-term changes in floodplain water level, we examined changes in the floodplain water table with a linear regression between year and annual 25th percentile river discharge (baseflow) at the mouth of Difficult Run (U.S. Geological Survey (USGS) gage #01646000) over the period of record (1935–2012).

Soil net N and P mineralization rates were measured monthly for 1 year (September 2008 to September 2009) using modified ion exchange resin cores [*Noe*, 2011] placed at each plot (detailed in *Noe et al*. [2013]). Inorganic nutrient loading to the soil surface was measured from concentrations in the uppermost resin bags. Soil cores in the mineralization study were also measured for soil bulk density, total carbon (TC), total nitrogen (TN), total phosphorus (TP), and texture.

2.4. Carbon Deposition and Erosion Measurements

Net sediment deposition over the study period was measured at each plot using artificial feldspar clay marker horizons. The depth of sediment over each marker horizon was measured routinely from 2008 through 2011 (detailed in *Schenk et al*. [2012] and *Hupp et al*. [2013]). In August 2011, sediment cores were taken over the marker horizon in the plots using 7.6 cm diameter PVC pipes. Two cores were taken over each marker horizon, and then each sediment core was extruded, the depth of new sediment was measured at four locations on the core, and the deposited sediment was separated from the feldspar in the field. In the lab, sediment samples were dried, weighed, and ground to 1 mm. Bulk density (g cm^{-3}) was calculated as dry mass per known volume of the sample. Sediment accretion rate (cm yr^{-1}) was calculated as the depth of sediment divided by deployment time, and mass sedimentation rate (g m^{-2} yr^{-1}) was calculated as the mass of sediment deposited divided by core area and deployment time. Subsamples of the dried samples were analyzed for TC and TN using a CHN analyzer (Thermo Scientific Flash 2000, Waltham, MA, USA). Separate subsamples were vapor digested with HCl to remove the mineral C, then combusted for total organic carbon (TOC) [*Hedges and Stern*, 1984]. Carbonates were not present in these soils, and we hereafter use TC but consider it to be TOC. Total P was also measured by acid-assisted microwave digestion (HNO_3 + HF; Mars 5, CEM Corp., Matthews Arm, NC, USA) followed by ICP-OES analysis (Perkin-Elmer Optima; Waltham, MA, USA). The C, N, and P sedimentation rates were calculated as the TC, TN, and TP concentration multiplied by mass sedimentation rate. The total organic fraction was determined by loss on ignition (LOI; 400°C for 16 h [*Nelson and Sommers*, 1996]), and organic and mineral sedimentation were similarly calculated.

Bank erosion was measured beginning in 2008 from three horizontal bank pins (1 m long) placed at each site at the ends of the three floodplain transects and two additional intermediary transects on both sides of the banks ($n = 30$ pins for each site, detailed in *Hupp et al*. [2013]). Pins were measured annually and after storm events. Net bank erosion rates (cm yr^{-1}) for each bank section (upper, middle, and lower) were calculated as the change in exposed pin length divided by deployment time. In June and July 2012, banks were cored horizontally to 5 cm depth near the pins using 7.6 cm diameter PVC tubes. Bank samples were wet sieved to 2 mm and dried to determine bulk density, then ground to 1 mm and analyzed for TC and LOI. Bank net mass, C, and organic and mineral erosion rates were calculated similar to floodplain sedimentation.

Duplicate litterfall traps were placed at each plot, 1.2 m above the soil surface with a surface area of 0.3 m^2. Litter was collected monthly for 1 year (2008–2009) as well as triplicate clip plots of peak herbaceous biomass (1 m^2; July 1 to August 10, 2009). The TC, TN, and TP concentrations of the ground vegetation were analyzed similar to soil cores and used to calculate litterfall and herbaceous carbon and nutrient fluxes (N. B. Rybicki et al., manuscript in preparation, 2015), referred to as vegetation C, N, and P flux. The vegetation C flux from litterfall and herbaceous matter is also referred to as aboveground production in the C budget.

©2014. American Geophysical Union. All Rights Reserved.

2.5. Carbon Budget

Measured carbon fluxes were used to develop a carbon budget for these floodplain wetland soils. Total soil CO_2 flux includes both heterotrophic respiration and autotrophic root respiration, which we did not distinguish in our study. To estimate the contribution of root respiration to total soil CO_2 emissions, we used a proportional value of 42% for temperate broadleaf forests derived from an extensive literature review of CO_2 flux partitioning [*Subke et al.*, 2006]. We did not measure belowground production but assumed it to be steady state for the duration of our sampling. Autochthonous contributions to the total C sedimentation rate were estimated from total vegetation (tree litterfall and herbaceous) litter C flux corrected for decomposition of each annual litter cohort over the study period, calculated from litterfall decay rates ($k = -1.01$) in southeastern U.S. forested wetlands [*Lockaby and Walbridge*, 1998]. Heterotrophic respiration was then divided into fluxes derived from autochthonous litter C decomposition in surface layers and decomposition of deeper soil C (calculated as residual CO_2 flux after accounting for estimates of root respiration and autochthonous litter C decomposition). Allochthonous C inputs were calculated as the total C sedimentation rate minus autochthonous C inputs corrected for decomposition. The net soil C flux could then be calculated:

$$\frac{dC}{dt} = C_{sed} - R_H - C_{er} - R_{CH_4} \tag{2}$$

where $\frac{dC}{dt}$ = the net gain or loss of C over time, C_{sed} = the total C sedimentation rate from allochthonous and decomposition-corrected autochthonous aboveground inputs over the feldspar pads, R_H = aerobic heterotrophic respiration in soil (root respiration removed), C_{er} = C erosion from banks (calculated over floodplain area), and R_{CH_4} = CH_4-C flux from anaerobic respiration. Units are in g C m^{-2} yr^{-1} with scaling of average instantaneous gas fluxes (s^{-1}) to an annual basis.

We also estimated the total C stock of Difficult Run floodplain soils to put our C balance into perspective. TC values per volume (g C cm^{-3}) have been measured at four floodplain depths spanning the entire height of the floodplain: surficial 5 cm soils from the mineralization study [*Noe et al.*, 2013] and upper, middle, and lower bank pin cores. A mean of TC values weighted by depth (1.1% C) was multiplied by the mean depth of floodplain soil among sites (1.4 m) to estimate the mean areal C stock of the floodplain soil (g C m^{-2}).

2.6. Statistics

The longitudinal, lateral, and temporal differences in CO_2, CH_4, and N_2O fluxes were tested using a repeated measure analysis of variance (RM-ANOVA; SAS 9.1), with longitudinal and lateral position, and their interaction, as factors and time as the repeated measure. The effects of the interaction of time with lateral and longitudinal position were both included in the models; however, their three-way interaction was not included because these fully factorial models underperformed the two-way factorial models based on Akaike Information Criteria indices. Significances along lateral or longitudinal gradients in the RM-ANOVA results were further evaluated using Tukey's post hoc tests with the Bonferroni correction; site 4 was eliminated from post hoc tests because of the lack of toe slope. Relationships between annual mean CO_2, CH_4, and N_2O fluxes and the suite of ecosystem variables were also analyzed using Pearson product-moment correlations (SPSS 13). Each gas flux was compared to the concurrent period of measurement of ecosystem variables for that gas. All nonnormal variables were transformed as appropriate, and all statistical tests used $\alpha = 0.05$. Weak correlations are indicated for $0.05 < P < 0.1$.

3. Results

3.1. Spatiotemporal Variation in Soil CO_2, CH_4, and N_2O Fluxes

Soil CO_2 and CH_4 fluxes differed significantly along lateral and longitudinal floodplain geomorphic gradients, depending on the time of year for CO_2 (Tables 1 and 2). N_2O fluxes averaged zero over all sampling locations and did not differ significantly along spatial nor temporal gradients (Table 2). Soil CO_2 fluxes over the 2 years of measurement ranged from 0.04 μmol m^{-2} s^{-1} in the backswamp at site 4 during winter to 8.8 μmol m^{-2} s^{-1} in the levee at site 2 during summer. Along the lateral geomorphic gradient, CO_2 fluxes were higher in the dry levees relative to both the backswamps and toe slopes, but there were no differences between backswamp and toe slope rates (Figure 2a). Conversely, CH_4 fluxes over the year of measurement were higher in the backswamps and toe slopes than the dry levees; backswamp and toe slope rates also did not differ from each other (Figure 2b).

©2014. American Geophysical Union. All Rights Reserved.

Table 1. Mean CO_2 Fluxes and Associated Ecosystem Variables Along Lateral and Longitudinal Gradients, and *P* Values of Repeated Measures ANOVAs Testing the Effects of Sampling Event (Time), Longitudinal Position, Lateral Geomorphic Position, and Their Interaction[a]

Term	CO_2 Flux (μmol CO_2 m^{-2} s^{-1})	pH	Soil Temperature (°C)	Water-Filled Pore Space (%)
		All Plots Mean		
All plots	3.1 ± 0.1 (664)	5.3 ± 0 (655)	12.4 ± 0.3 (661)	57.5 ± 0.8 (657)
		Longitudinal Gradient Means		
Site 0	3.1 ± 0.3 (114)	4.9 ± 0.0 (114)	13.0 ± 0.8 (114)	46.1 ± 1.8 (114)
Site 1	3.0 ± 0.2 (127)	5.2 ± 0.1 (127)	11.9 ± 0.7 (124)	50.6 ± 1.7 (127)
Site 2	3.6 ± 0.3 (111)	5.3 ± 0.0 (112)	12.2 ± 0.7 (112)	59.3 ± 1.6 (113)
Site 3	2.8 ± 0.2 (129)	5.4 ± 0.0 (123)	12.7 ± 0.7 (129)	64.9 ± 1.5 (123)
Site 4	3.7 ± 0.5 (60)	5.4 ± 0.0 (57)	13.5 ± 1.2 (59)	55.7 ± 3.4 (58)
Site 5	2.6 ± 0.2 (123)	5.5 ± 0.0 (122)	11.6 ± 0.7 (123)	66.9 ± 1.7 (122)
		Lateral Gradient Means		
Levee	3.6 ± 0.2 (241)	5.5 ± 0.0 (238)	12.3 ± 0.5 (239)	47.6 ± 1.1 (238)
Backswamp	2.7 ± 0.2 (220)	5.3 ± 0.0 (216)	12.7 ± 0.6 (218)	63.6 ± 1.3 (218)
Toe slope	2.8 ± 0.2 (203)	5.0 ± 0.0 (201)	12.1 ± 0.6 (204)	62.6 ± 1.5 (201)
		Repeated Measures ANOVA P Values		
Time	**<0.001**	**<0.001**	**<0.001**	**<0.001**
Longitudinal	**<0.001**	**<0.001**	**<0.001**	**<0.001**
Lateral	**<0.001**	**<0.001**	0.229	**<0.001**
Lateral × longitudinal	**<0.001**	**<0.001**	**<0.001**	**<0.001**
Longitudinal × time	**<0.001**	**<0.001**	**<0.001**	*0.061*
Lateral × time	0.372	0.154	0.412	0.765

[a]Means reported as mean ± one S.E. (*n*). Results of $P < 0.05$ highlighted in bold and $P < 0.10$ highlighted in italics.

Longitudinally, site 2 had higher CO_2 fluxes than sites 0, 1, 3, and 5, which were not significantly different from each other, but only in the levee and backswamp (Figure 2a). CO_2 fluxes at site 4 also appear high, but this was our wettest site, where measurements could not be made when surface water surface was deeper than the top of the collar. This happened often at backswamp locations at site 4 during colder months (leaf off), biasing measurements to dry and warm summer rates during the first year. CH_4 emission rates were negative at all sites except site 4, indicating the oxidation of atmospheric methane by most of these floodplain soils (Figure 2b). Site 0 had greater CH_4 consumption than the other sites (site 4 had positive emission rates but was excluded from post hoc analyses due to lack of a toe slope).

However, the effect of lateral geomorphic gradients depended on longitudinal watershed position for CO_2, as shown by their significant interaction (Table 1). Emission rates of CO_2 from toe slope soils were greatest and larger than either levee or backswamp at site 0 but generally decreased in the toe slope at more downstream sites (Figure 2a). CO_2 fluxes also varied significantly with sampling event; fluxes were highest in summer (6.1 ± 0.1 μmol m^{-2} s^{-1}) and lowest in winter (0.7 ± 0.0 μmol m^{-2} s^{-1}). Spring and fall fluxes (2.6 ± 0.2 and 2.8 ± 0.1 μmol m^{-2} s^{-1}, respectively) were significantly lower than summer fluxes and significantly higher than winter fluxes, but spring and fall fluxes did not differ from each other. Sampling period did not affect CH_4 fluxes.

3.2. Spatiotemporal Variation in Associated Variables: Soil Moisture, Temperature, and pH

Soil water-filled pore space (WFPS), temperature, and pH also varied significantly along lateral, longitudinal, and temporal floodplain gradients (Tables 1 and 2). Over the 2 years, the natural, high-elevation levees along the stream channel were significantly drier than backswamps and toe slopes, which did not differ in wetness (Figure 3). Headwater sites 0 and 1 have less hydrologic connection (e.g., deeper groundwater, shorter hydroperiods) than sites farther downstream and were thus significantly drier than sites 2, 3, and 5; site 2 was also significantly drier than sites 3 and 5. However, lateral geomorphic differences were dependent upon longitudinal position for WFPS, and vice versa. Generally, plots became wetter farther downstream and away from the levees. Among all plots, annual mean WFPS ranged from 20.4% at the levee of site 4 to 89.9% at the backswamp of site 4. WFPS also differed temporally, with plots being significantly drier in summer (43.0 ± 1.4%) than in winter, spring, and fall (64.9 ± 1.4, 63.6 ± 1.5%, and 59.1 ± 1.4%, respectively), but time did not influence spatial differences in WFPS.

©2014. American Geophysical Union. All Rights Reserved.

Table 2. Mean CH_4 and N_2O Fluxes and Associated Ecosystem Variables Along Lateral and Longitudinal Gradients, and *P* Values of Repeated Measures ANOVAs Testing the Effects of Sampling Event (Time), Longitudinal Position, Lateral Geomorphic Position, and Their Interaction[a]

Term	CH_4 Flux (μmol CH_4 m^{-2} s^{-1})	N_2O Flux (μmol N_2O m^{-2} s^{-1})	pH	Soil Temperature (°C)	Water-Filled Pore Space (%)
		All Plots Mean			
All plots	−0.0007 ± 0.0002 (135)	0 ± 0 (136)	5.1 ± 0 (132)	12.2 ± 0.7 (131)	53.4 ± 3.5 (131)
		Longitudinal Gradient Means			
Site 0	−0.0022 ± 0.0007 (24)	0 ± 0.0001 (24)	4.8 ± 0.1 (24)	12.5 ± 1.7 (24)	48.9 ± 6.7 (24)
Site 1	−0.0005 ± 0.0003 (24)	0.0001 ± 0.0001 (24)	5 ± 0.1 (24)	12.1 ± 1.8 (21)	52.4 ± 8.1 (23)
Site 2	−0.0007 ± 0.0003 (24)	0 ± 0 (24)	5.2 ± 0.1 (24)	10.9 ± 1.6 (22)	49.3 ± 5.6 (23)
Site 3	−0.0008 ± 0.0004 (24)	0 ± 0.0001 (24)	5.2 ± 0.1 (22)	12.8 ± 1.7 (24)	49.5 ± 6.4 (22)
Site 4	0.0011 ± 0.0013 (16)	0.0001 ± 0.0001 (16)	5.2 ± 0.1 (14)	13.1 ± 2.7 (16)	77.4 ± 20.5 (15)
Site 5	−0.0005 ± 0.0005 (23)	0 ± 0.0001 (24)	5.3 ± 0 (24)	11.7 ± 1.7 (24)	51.4 ± 6 (24)
		Lateral Gradient Means			
Levee	−0.0016 ± 0.0005 (48)	0 ± 0 (48)	5.3 ± 0.1 (46)	12 ± 1.3 (47)	38.8 ± 3.8 (45)
Backswamp	0 ± 0.0005 (48)	0.0001 ± 0.0001 (48)	5.1 ± 0 (47)	12.4 ± 1.3 (44)	60.2 ± 7.1 (47)
Toe slope	−0.0005 ± 0.0002 (39)	−0.0001 ± 0 (40)	4.9 ± 0.1 (39)	12 ± 1.3 (40)	62.1 ± 6.2 (39)
		Repeated Measures ANOVA P values			
Time	0.952	0.173	**0.007**	**<0.001**	**<0.001**
Longitudinal	**0.012**	0.898	**<0.001**	**<0.001**	**0.043**
Lateral	**0.006**	0.108	**<0.001**	0.226	**<0.001**
Lateral × longitudinal	0.270	0.258	**<0.001**	0.154	**0.005**
Longitudinal × time	*0.098*	0.562	0.864	**<0.001**	0.772
Lateral × time	0.363	0.938	*0.062*	0.526	0.432

[a]Means reported as mean ± one S.E. (*n*). Results of $P < 0.05$ highlighted in bold and $P < 0.10$ highlighted in italics.

Our Difficult Run floodplain plots were relatively dry; soil WFPS was greater than 90% only 7% of the time during the 2 years of study. Furthermore, the average hydroperiod (percent of time with surface water) for all plots was only 2.9%; the greatest average hydroperiod was 66% for one backswamp plot at site 4, but 10 plots never had standing water. After removing three outlier wet years (1979, 1996, and 2003) from the 78 year record of river discharge at the mouth of Difficult Run, we also found a very weak decreasing trend in low-flow (25th quartile) discharges over time (Pearson product-moment correlation, $n = 75$, $r = -0.203$, $P = 0.080$; Figure 4).

Soil temperature varied with time as expected. Temperature also varied significantly with longitudinal position; sites 0 and 3 had significantly warmer soil than sites 1, 2, and 5, but these longitudinal differences were dependent upon time of year. Soil pH varied along lateral and longitudinal gradients (and their interaction) and through time. Generally, soil pH was higher in levees and increased in downstream sites, particularly for levees and toe slopes. The levee and toe slope at site 0 and the toe slope at site 1 had the lowest soil pH values; spatial differences did not depend on sampling period for pH.

3.3. Ecosystem Controls on Soil Greenhouse Gas Fluxes

Spatial variation in soil GHG fluxes in general varied with oxygen availability along gradients in soil texture and wetness (Table 3). For all plots, annual soil CO_2 flux was most strongly correlated with soil WFPS ($r = -0.379$, Figure 5) and mass of deposited mineral sediment ($r = 0.448$). Annual CO_2 fluxes also increased weakly with sediment accretion rate, sedimentation rate, sediment coarse-sand fraction, and soil percent nitrification [net nitrification÷(ammonification + nitrification)], and decreased with soil WFPS, soil fine sand fraction, and sediment bulk density. Mean CO_2 fluxes did not depend on sedimentation, soil, or vegetative C, N, or P concentrations or fluxes. CO_2 fluxes were negatively correlated with C:N and weakly correlated with C:P ratios of deposited sediment. There were no strongly significant relationships among annual mean CO_2, CH_4, and N_2O fluxes (Table 3). For example, there was no significant association between CO_2 and CH_4 fluxes ($r = 0.081$, $P = 0.649$); however, there was a very weak positive association between CH_4 and N_2O fluxes ($n = 34$, $r = 0.294$, $P = 0.092$). Temporal variation in intra-annual CO_2 flux was positively correlated with soil temperature ($n = 658$, $r = 0.871$, $P < 0.001$), soil redox ($n = 604$, $r = 0.284$, $P < 0.001$), and soil pH ($n = 652$, $r = 0.129$, $P = 0.001$) and negatively correlated with soil WFPS ($n = 654$, $r = -0.441$, $P < 0.001$).

Spatial differences in annual CH_4 fluxes varied positively with the ecosystem moisture variables of hydroperiod and soil WFPS. Variables indirectly linked to moisture gradients were also positively linked to CH_4 fluxes, including P sedimentation rate, ammonium (NH_4^+) loading to the surface, and soil net N

©2014. American Geophysical Union. All Rights Reserved.

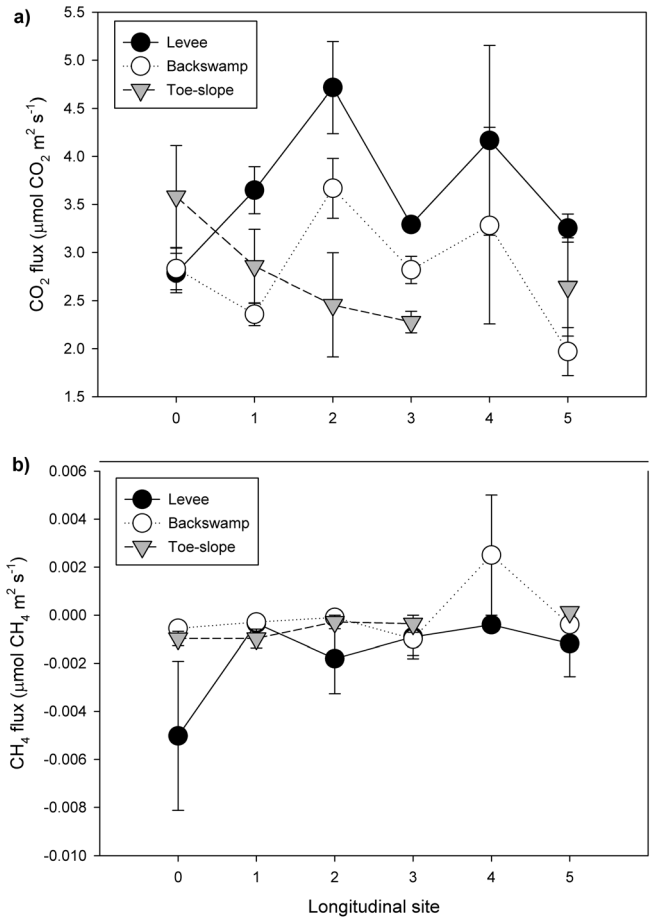

Figure 2. Lateral and longitudinal variation in soil (a) CO_2 emission rates and (b) CH_4 emission rates. Bars represent 1 SE.

mineralization, and weakly to soil ammonification rate and nitrate (NO_3^-) loading to the surface. Soil texture impacted CH_4 fluxes similar to moisture variables, indicating CH_4 emission rates were controlled by lack of available oxygen. CH_4 fluxes increased with soil clay fraction and decreased with soil median particle size (D50), mean size, and silt fraction. CH_4 fluxes were also not correlated with inputs of C and N from vegetation or sedimentation but were negatively correlated with litter C:N and C:P ratios, sediment N:P and weakly with sediment C:N and C:P ratios. Among all measured ecosystem controls, annual CH_4 flux was most strongly correlated with soil clay fraction ($r = 0.567$). Temporal differences in CH_4 fluxes were most strongly correlated with soil WFPS ($n = 128$, $r = 0.242$, $P = 0.006$). While N_2O fluxes were very low and averaged zero over the year, annual fluxes showed some weak associations with moisture variables. N_2O flux positively correlated most strongly with sedimentation rate ($r = 0.341$) and increased weakly with hydroperiod, sediment accretion rate, and P sedimentation rate; soil redox had a weak negative effect. N_2O flux did not correlate with N mineralization rate or % nitrification.

3.4. Carbon Balance

All six floodplain sites showed a negative C balance (Table 4), indicating that these floodplain wetland soils are currently a net source of carbon to the atmosphere. The net loss from all sites is 338 g C m^{-2} yr^{-1} calculated as a simple average of all sites (Table 4 and Figure 6). The mean total C stock of the floodplain soils is 20.5 kg C m^{-2}; the C balance indicates that the floodplain is losing approximately 1.7% of stored soil carbon per year. Site 2 was the greatest source of carbon per area of floodplain, due partly to its relatively high CO_2 flux and C bank erosion rates and relatively low sediment C deposition rates. CO_2 fluxes as soil heterotrophic and root respiration were the largest C flux in the budget, while CH_4 oxidation (incorporated as CO_2 flux) represented a very small portion of C cycling in this floodplain. Bank erosion was a relatively minor source of C loss by the floodplain. Over all of the sites, allochthonous riverine C accounted for about 66% of net carbon deposited on the floodplain with the remainder from autochthonous inputs after accounting for litter decomposition. On average, allochthonous C deposition exceeded bank C erosion, indicating that the floodplain was a fluvial sink of particulate organic C.

4. Discussion

4.1. Total GHG Fluxes

Our mean annual floodplain soil CO_2 emissions (1091 ± 54 g C m^{-2} yr^{-1}) were higher than those reported in the global soil respiration database for wetlands (344 ± 278 g C m^{-2} yr^{-1}) but were similar to uplands (816 ± 516 g C m^{-2} yr^{-1} [*Bond-Lamberty and Thomson*, 2010]). Mean CO_2 emissions in the Difficult Run

©2014. American Geophysical Union. All Rights Reserved.

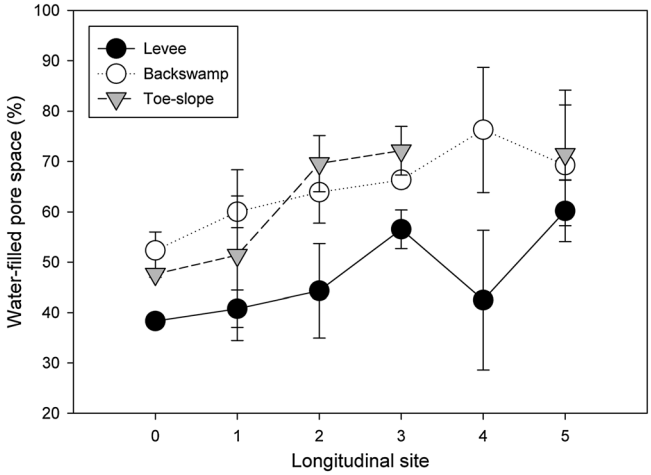

Figure 3. Lateral and longitudinal variation in water-filled pore space. Bars represent 1 SE.

floodplain (Table 4) were comparable to tropical Amazon floodplains (1300 g C m^{-2} yr^{-1} [*Richey et al.*, 1988], Coastal Plain dry forests and forested wetlands in North Carolina (1129 g C m^{-2} yr^{-1} [*Morse et al.*, 2012]; 960–1103 g C m^{-2} yr^{-1} [*Miao et al.*, 2013]), a gum swamp in North Carolina (1088 g C m^{-2} yr^{-1} [*Bridgham and Richardson*, 1992]), the upland-swamp transition zone in a Louisiana bottomland hardwood forest (909 g C m^{-2} yr^{-1} [*Yu et al.*, 2008]), and floodplain wetlands in Georgia (919 g C m^{-2} yr^{-1} [*Pulliam*, 1993]). Rates were in agreement with other floodplain or transition wetlands in the southeast, which may be higher than global averages dominated by cooler northern peatlands. For example, CO_2 emission rates averaged only 30 g C m^{-2} yr^{-1} in an Alaskan wet sedge floodplain [*Giblin et al.*, 1991].

Atmospheric CH_4 emissions due to methanogenesis were not a significant contributor to GHG emissions in these floodplains. CH_4 fluxes mostly did not differ from zero but were on average slightly negative, indicating that methane is consumed. Typical wetland methane emissions average 77 g C m^{-2} yr^{-1} [*Morse et al.*, 2012], while ours were −0.3 g C m^{-2} yr^{-1}. Our rates are not unprecedented; rates of 0.8–1.0 g CH_4-C m^{-2} yr^{-1} were found in tidal areas along the Savannah River, Georgia [*Krauss and Whitbeck*, 2012]. Areas with unsaturated surface soils could oxidize CH_4 [*Le Mer and Roger*, 2001], and the Difficult Run floodplain is not typically flooded when soils are warmest and microbial activity greatest. Zero emissions and net methane oxidation are common in other wetlands with lowered water tables or in nonflooded zones [*Harriss et al.*, 1982; *Boon et al.*, 1997; *Wickland et al.*, 1999; *Updegraff et al.*, 2001; *Couwenberg et al.*, 2010; *Samaritani et al.*, 2013]. Laboratory incubations of Australian floodplain soil showed that potential CH_4 oxidation was an order of magnitude higher than potential methanogenesis [*Boon and Lee*, 1997], indicating that aeration of sediments could limit CH_4 emissions. Intermittently flooded zones in an Ohio created riparian wetland showed a 30% reduction in CH_4 emissions when compared to the permanently flooded zones [*Altor and Mitsch*, 2006].

Our methane fluxes were very small on average, though it is possible that our sampling methods underestimated methane flux. Large proportions of CH_4 fluxes to the atmosphere are known to be transported through aerenchymal tissues in plants [*Terazawa et al.*, 2007; *Koh et al.*, 2009], which provide a diffusive pathway from deeper anaerobic soil layers. Plant transport has been shown to account for 91% of CH_4 emissions in the Florida Everglades [*Whiting et al.*, 1991], and vegetation increased emissions 5 times over bare soils in tropical Orinoco floodplains [*Smith et al.*, 2000]. However, *Altor and Mitsch* [2006] did not find significant differences in CH_4 emissions between vegetated and nonvegetated plots in Ohio created riparian wetlands. Our gas sampling did not include vegetation, though our fluxes were so low that they may not be significant even when accounting for plant transport.

Ebullition, the sudden release of methane bubbles, has been demonstrated as another major pathway for CH_4 emission to the atmosphere in wetlands [*Bartlett et al.*, 1990; *Pulliam*, 1993]. In a small UK lake, ebullition accounted for 96% of CH_4 emissions, with large bursts of CH_4 occurring during periods of low atmospheric pressure [*Casper et al.*, 2000]. With sampling each location only 4 times per year, it is possible that we may not have captured some of these large periodic fluxes. However, with inundation occurring on average 3% of the time, ebullition is not likely a common occurrence in this floodplain.

The floodplain contributed zero N_2O to the atmosphere on average. While anaerobic denitrification and aerobic nitrification both potentially produce N_2O [*Freeman et al.*, 1997], denitrification is considered to produce more N_2O in wetlands [*Davidson et al.*, 2000]. In this study, N_2O emissions correlated neither with N mineralization nor percent nitrification, supporting the hypothesis that denitrification is the greater source of

©2014. American Geophysical Union. All Rights Reserved.

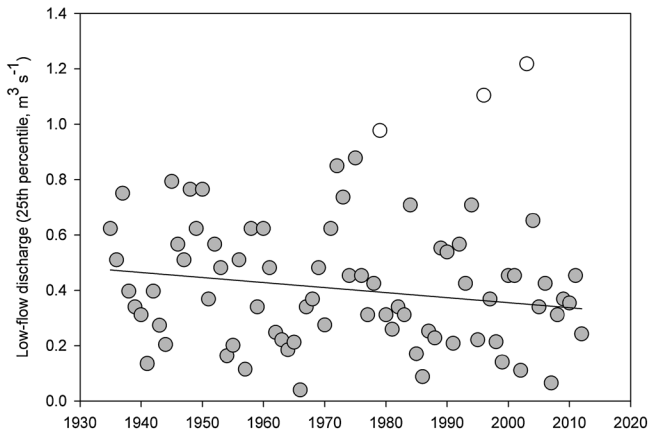

Figure 4. Regression of 25th percentile annual discharge in Difficult Run versus year, 1935–2012. Outlier years are shown as open symbols.

N_2O in wetlands. Dry conditions in these wetlands are likely not favorable for denitrification and result in the net production of soil nitrate [*Noe et al*., 2013], but denitrification may have been enhanced during short periods of inundation [*Sánchez-Andrés et al*., 2010], and periodic high N_2O fluxes may not have been captured during our seasonal sampling. Regardless, wetlands that are not polluted and enriched with N are not considered to be a major contributor to global N_2O emissions [*Bridgham et al*., 2006].

Aerobic respiration and anaerobic methanogenesis and fermentation are opposing processes, with the former likely to dominate in oxidizing soil conditions and the latter more important in reducing soils [*Crill*, 1991]. There were no relationships between CO_2, CH_4, or N_2O fluxes in this study. CO_2 and CH_4 emissions were not significantly correlated in created Ohio riparian wetlands [*Altor and Mitsch*, 2008] nor northern Minnesota wetlands [*Bridgham et al*., 1998]. *Bridgham et al*. [1998] suggested that methanogenic microbes may utilize different substrates than aerobic heterotrophs. CO_2 fluxes may also be dominated by root respiration, and CH_4 fluxes dominated by microbial respiration. The lack of association between anaerobic CH_4 and N_2O emissions could be due to small differences in the atmospheric and soil concentrations of each gas [*Yu et al*., 2008] or the lack of a eutrophic environment for promoting denitrification.

4.2. Spatiotemporal Variation in GHG Fluxes

CO_2 and CH_4 fluxes both varied along lateral and longitudinal gradients in floodplain hydrologic connectivity. CO_2 emissions also varied seasonally and with the interaction between lateral geomorphology and longitudinal watershed position. CH_4 emissions did not fluctuate seasonally, and N_2O fluxes showed neither spatial nor temporal patterns. These longitudinal and lateral changes in emissions are concordant with gradients in floodplain hydrology, geomorphology, and soils. In general, soils at headwater sites along Difficult Run are more organic and higher in nutrient concentrations with lower bulk density than downstream sites [*Noe et al*., 2013], which have greater hydrologic connectivity (greater flood frequency, magnitude, and duration with greater mineral sediment inputs) [*Hupp et al*., 2013]. Levees are higher in elevation with less hydrologic connectivity but higher mineral sedimentation rates than other lateral geomorphic units. Soil texture is similar along lateral and longitudinal gradients, but there is greater organic and N content toward backswamps and toe slopes [*Noe et al*., 2013].

Variations in soil CO_2 emissions along lateral and longitudinal gradients are likely due to differences in hydrologic connectivity, which in turn alter lateral and longitudinal geomorphology and soil moisture [*Welti et al*., 2012]. CO_2 emissions were highest on drier levees relative to wetter backswamps; such spatial patterns of CO_2 emissions increasing along hydrologic gradients from wet to dry have been well established in floodplain wetlands [*Yu et al*., 2008; *Welti et al*., 2012], southern forested wetlands [*Koh et al*., 2009; *Morse et al*., 2012; *Miao et al*., 2013], and northern and Arctic peatlands [*Sjögersten et al*., 2006; *Jaatinen et al*., 2008]. Along the longitudinal gradient, CO_2 emissions generally but sporadically decreased from dry headwaters to wetter downstream sites (see Figure 3), but only site 2 had significantly higher emission rates than the other sites. Site 2 is among the drier headwater sites, but sites 0 and 1 are significantly drier. Site 2 differs from other sites along the longitudinal gradient in that it has reduced deposition, shallower legacy sediment, greater bank erosion, and lower sinuosity [*Hupp et al*., 2013], which contribute to the uniqueness of the site.

Soil CO_2 emissions also varied temporally, with highest rates in summer, followed by spring and autumn, which were higher than winter. Intra-annual variations were strongly dependent on seasonal changes in soil temperature, soil pH, and soil redox. Hydrologic patterns also vary seasonally, with this floodplain being

©2014. American Geophysical Union. All Rights Reserved.

Table 3. Pearson Product-Moment Correlations ($n = 34$) Between Soil Gas Fluxes and Potential Ecosystem Controls[a]

Variables	Statistic	CO_2 Flux	CH_4 Flux	N_2O Flux	Variables	Statistic	CO_2 Flux	CH_4 Flux	N_2O Flux
CO_2 flux	*r*		0.081	−0.004	Litterfall C production rate	*r*	−0.115	−0.062	−0.005
	P		0.649	0.981		*P*	0.516	0.728	0.979
CH_4 flux	*r*			*0.294*	Litterfall N production rate	*r*	−0.179	0.207	−0.060
	P			*0.092*		*P*	0.312	0.240	0.738
Water level 2012	*r*	−0.239	0.168	0.230	Litterfall P production rate	*r*	−0.280	0.195	−0.062
	P	0.173	0.343	0.191		*P*	0.108	0.268	0.728
Hydroperiod	*r*	−0.054	**0.381**	*0.312*	Herbaceous C production rate	*r*	−0.043	0.171	0.186
	P	0.764	**0.026**	*0.073*		*P*	0.811	0.333	0.291
Soil redox	*r*	−0.171	0.025	*−0.206*	Herbaceous N production rate	*r*	−0.061	0.151	0.162
	P	0.333	0.836	*0.076*		*P*	0.734	0.394	0.359
Soil WFPS	*r*	**−0.379**	**0.383**	0.046	Herbaceous P production rate	*r*	−0.080	0.211	0.156
	P	**0.027**	**0.025**	0.796		*P*	0.651	0.230	0.378
Soil pH	*r*	0.200	0.037	0.166	Litterfall C:N	*r*	0.039	**−0.364**	0.001
	P	0.256	0.833	0.348		*P*	0.825	**0.034**	0.996
Soil temperature	*r*	−0.144	0.143	0.195	Litterfall C:P	*r*	0.060	**−0.387**	0.013
	P	0.417	0.421	0.270		*P*	0.736	**0.024**	0.943
Soil bulk density	*r*	−0.135	−0.057	0.013	Litterfall N:P	*r*	0.130	0.020	0.044
	P	0.447	0.749	0.941		*P*	0.463	0.912	0.805
Soil d50	*r*	−0.192	**−0.516**	−0.021	Sedimentation rate	*r*	*0.316*	0.230	**0.341**
	P	0.276	**0.002**	0.905		*P*	*0.069*	0.190	**0.049**
Soil coarse-sand fraction	*r*	0.204	−0.025	0.063	C sedimentation rate	*r*	0.100	0.140	0.181
	P	0.247	0.889	0.723		*P*	0.572	0.431	0.305
Soil fine sand fraction	*r*	**−0.346**	−0.260	0.031	N sedimentation rate	*r*	0.190	0.253	0.256
	P	**0.045**	0.137	0.862		*P*	0.281	0.149	0.144
Soil silt fraction	*r*	0.197	**−0.342**	−0.154	P sedimentation rate	*r*	0.241	**0.351**	*0.317*
	P	0.265	**0.047**	0.383		*P*	0.170	**0.042**	*0.068*
Soil clay fraction	*r*	0.079	**0.567**	0.024	Sediment C:N	*r*	**−0.367**	*−0.326*	−0.184
	P	0.659	**<0.001**	0.894		*P*	**0.046**	*0.079*	0.330
Soil TC	*r*	−0.166	0.131	0.008	Sediment C:P	*r*	*−0.353*	*−0.340*	−0.178
	P	0.348	0.460	0.963		*P*	*0.055*	*0.066*	0.346
Soil TN	*r*	−0.156	0.144	−0.081	Sediment N:P	*r*	−0.156	**−0.368**	−0.262
	P	0.378	0.417	0.650		*P*	0.412	**0.046**	0.161
Soil TP	*r*	−0.188	0.273	−0.200	Sediment mineral fraction	*r*	**0.448**	0.241	*0.360*
	P	0.288	0.118	0.258		*P*	**0.013**	0.199	*0.050*
Soil NH_4^+ mineralization rate	*r*	−0.212	*0.315*	0.099	Sediment d50	*r*	0.231	−0.119	**0.373**
	P	0.228	*0.070*	0.579		*P*	0.220	0.531	**0.042**
Soil NO_3^- mineralization rate	*r*	0.043	0.059	−0.129	Sediment coarse-sand fraction	*r*	*0.349*	−0.206	0.098
	P	0.808	0.739	0.466		*P*	*0.059*	0.276	0.606
Soil net N mineralization rate	*r*	−0.005	**0.417**	0.075	NO_3^- loading rate	*r*	0.118	*0.306*	−0.138
	P	0.979	**0.014**	0.673		*P*	0.506	*0.078*	0.436
Soil percent nitrification	*r*	*0.306*	−0.153	−0.077	NH_4^+ loading rate	*r*	0.016	**0.370**	0.193
	P	*0.078*	0.388	0.663		*P*	0.929	**0.031**	0.273
Soil P mineralization rate	*r*	**−0.364**	0.317	−0.019	PO_4^{3-} loading rate	*r*	*−0.293*	0.003	−0.206
	P	**0.041**	0.077	0.918		*P*	*0.093*	0.988	0.242

[a]Correlations with $P < 0.05$ highlighted in bold and $P < 0.10$ highlighted in italics.

wettest in winter and spring and driest in summer. Soil temperature and hydrology likely interact to create the significant interactions between season and lateral and geomorphic gradients in these sites. In the Hubbard Brook Experimental Forest, soil respiration was faster in warmer, drier sites along an elevation gradient [*Groffman et al.*, 2009]. The interaction between soil temperature and quantity of organic matter explained most seasonal and spatial patterns in dry site CO_2 emissions in a southeastern U.S. forested floodplain [*Pulliam*, 1993]; although spatial patterns in temperature and organic matter were not significant here, we did not measure seasonal changes in organic matter. On average, there is a latitudinal gradient in decomposition in freshwater wetlands, with faster rates at warmer lower latitudes [*Brinson et al.*, 1981].

Methane emission rates showed a reverse spatial pattern compared to CO_2; they were highest in backswamps and toe slopes and lowest in dry levees. Similar patterns of increasing methanogenesis and CH_4 emission along a hydrologic gradient of dry to wet sites has been observed in northern peatlands and

©2014. American Geophysical Union. All Rights Reserved.

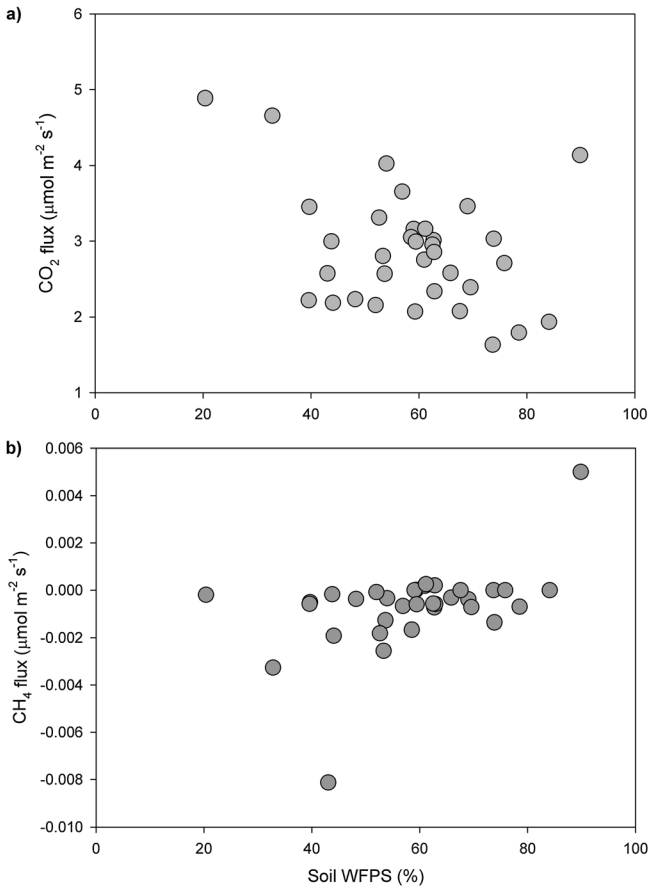

Figure 5. Average annual trends in soil (a) CO_2 emissions and (b) CH_4 emissions versus WFPS. $n = 34$ plots.

floodplains [*Moosavi and Crill*, 1997; *Gulledge and Schimel*, 2000; *Samaritani et al*., 2013] and temperate riparian wetlands [*Pulliam*, 1993; *Wickland et al*., 1999]. Along the longitudinal gradient, only site 0 showed higher rates of methane consumption on the drier levee, which is also more of a colluvial rather than alluvial feature at this site. Emission rates were positive only in the backswamp at site 4, which is more continually inundated than all other sites. CH_4 emission rates likely were not higher from site 4 because it is flooded during winter and spring, when temperatures are lowest. Thus, CH_4 emissions do not appear to vary seasonally.

4.3. Ecosystem Controls on GHG Fluxes

Annual average soil CO_2 fluxes correlated with ecosystem characteristics representing hydrologic conditions expressed over the lateral and longitudinal floodplain gradients. Rates were negatively correlated with soil wetness; as water levels and soil WFPS decrease, soils become more aerated and oxidizing aerobic respiration increases, stimulating CO_2 production. The link between increased CO_2 emission rates and decreased water tables has been demonstrated in northern peatlands and floodplains [*Moore and Knowles*, 1989; *Updegraff et al*., 1995; *Moore and Dalva*, 1997; *Gulledge and Schimel*, 2000; *Samaritani et al*., 2013] and temperate wetlands and floodplains [*Koh et al*., 2009; *Gallardo et al*., 2012; *Krauss and Whitbeck*, 2012; *Miao et al*., 2013]. However, in extreme dryness, respiration can become moisture limited, and respiration rates will increase with soil WFPS, such as in the tropics [*Gupta and Singh*, 1981; *Goulden et al*., 2004], boreal forests [*Wickland et al*., 2010], and semiarid floodplains [*Valett et al*., 2005]. In this study, we observed a linear increase in respiration with decreasing WFPS from 90% to 20%, indicating that microbial respiration was not limited by insufficient soil moisture. Intermittent flooding can also stimulate respiration rate and CO_2 fluxes, because floodwater delivers carbon substrates and nutrients to the floodplain and also relieves drought stress on microbes. Flood pulses have been shown to stimulate respiration [*Fromin et al*., 2010; *Sánchez-Andrés et al*., 2010; *Wilson et al*., 2011], and floods have substantially increased since urbanization of the Difficult Run watershed in the mid-1960s [*Hupp et al*., 2013], but they can also dampen decomposition and respiration with periodic returns to anaerobic conditions [*Brinson et al*., 1981]. Still, flood pulsing showed no effect on CO_2 emissions in created riparian wetlands in Ohio [*Altor and Mitsch*, 2008].

Several variables representing soil and sediment texture impacted CO_2 fluxes; fine textured soils are less oxygenated than coarse soils due to smaller pore space [*Groffman and Tiedje*, 1991]. CO_2 fluxes varied positively with coarse-sand content of deposited sediment and weakly with sediment mineral content and had a weak negative relationship with sediment bulk density. Coarse soil textures also allow maximum gas diffusion to the atmosphere [*Samaritani et al*., 2013].

Quality and quantity of soil organic matter substrate are also known to influence microbial respiration [*Bridgham and Richardson*, 1992; *Pulliam*, 1993; *Updegraff et al*., 1995], and sediment inputs are known to

©2014. American Geophysical Union. All Rights Reserved.

Table 4. Floodplain C Budget Showing Total Average and Longitudinal Differences in C Fluxes for Difficult Run Floodplains[a]

Site	CO_2	CH_4	Heterotrophic Respiration:Soil	Root Respiration	Aboveground Production	Heterotrophic Respiration:Litter	Total Sedimentation	Allochthonous Inputs	Bank Erosion	Net C Flux
Mean	−1091	0.3	−432	−458	240	−201	111	72	−17	−338
0	−1026	0.8	−414	−431	216	−182	146	111	−8	−277
1	−1018	0.2	−369	−427	264	−222	137	95	−18	−249
2	−1231	0.3	−536	−517	213	−178	48	14	−41	−529
3	−1087	0.3	−407	−457	267	−224	121	78	−13	−299
4	−1335	−0.4	−570	−561	243	−204	142	103	−18	−445
5	−929	0.2	−337	−390	241	−202	83	44	−5	−259

[a]All values are g C m^{-2} yr^{-1}. Positive fluxes indicate inputs, negative fluxes indicate losses.

stimulate biogeochemical processing along spatial gradients [*Noe et al.*, 2013]. C fluxes decreased significantly with distance from hydrologic and nutrient inflows in the Florida Everglades [*DeBusk and Reddy*, 2003], and high sedimentation locations in southeast coastal plain wetlands were drier with higher sand and lower organic matter content, reducing microbial processing [*Jolley et al.*, 2010]. In coastal freshwater swamps in Georgia, soil respiration was most strongly linked to root biomass and length [*Krauss et al.*, 2012]. We surprisingly did not find any correlations between CO_2 fluxes and soil, sediment, or vegetation C, N, or P pools or fluxes. We did not measure root biomass, but root C is included in measured soil TC. Thus, quantity of organic matter did not appear to regulate microbial respiration in the Difficult Run floodplain; the rates of heterotrophic respiration were highest at locations with more sand but were not influenced by C inputs, indicating that aeration was more important for aerobic respiration than organic matter availability in this floodplain. Furthermore, the lack of correlation between CO_2 flux and soil N mineralization rate is surprising because both are products of microbial decomposition of organic matter and suggests that gradients of net production of inorganic N were less influenced by microbial heterotrophic respiration than by N immobilization. CO_2 fluxes were negatively correlated with sediment C:N and C:P, suggesting possible nutrient limitations of microbial respiration where deposited organic sediment is more refractory than labile. However, differences in sediment nutrient stoichiometry may also covary with hydrologic gradients that directly influence decomposition rate.

Soil CH_4 fluxes showed the expected opposite pattern to CO_2 fluxes, increasing with variables that signified a wetter hydrology. Fluxes increased with soil WFPS and hydroperiod. Our sites nearly universally exhibited methane oxidation, which was shown to occur when WFPS reached below 40% in the prairie pothole region [*Gleason et al.*, 2009]. Methane oxidation was highest at our levee sites, which averaged 39% WFPS. CH_4 emission has been shown to increase with water table depth or soil water content in many studies in northern bogs and peatlands [*Moore and Knowles*, 1989; *Gulledge and Schimel*, 2000; *Updegraff et al.*, 2001], temperate wetlands and floodplains [*Pulliam*, 1993; *Koh et al.*, 2009], tropical wetlands [*Smith et al.*, 2000; *Couwenberg et al.*, 2010], and intermittently dry floodplains [*Boon et al.*, 1997]. Periodic flood pulses can also suppress CH_4 emissions [*Altor and Mitsch*, 2008].

CH_4 fluxes also correlated with variables that are linked to hydrologic connectivity of floodplains: in addition to hydroperiod and soil WFPS, P sedimentation, NH_4^+ loading, and NO_3^- loading all increase with flooding, and net N mineralization and ammonification are primarily anaerobic processes stimulated by flooding [*Noe et al.*, 2013]. However, NH_4^+ was shown to suppress CH_4 consumption by CH_4 oxidizers [*Le Mer and Roger*, 2001], which may be why oxidation rates (negative values) decreased with increasing NH_4^+ loading. Correlation patterns between CH_4 emissions and soil texture variables countered those for CO_2 fluxes: rates were strongly controlled by soil clay fraction and decreased with larger grain sizes. Smaller grain sizes limit available oxygen and increase

©2014. American Geophysical Union. All Rights Reserved.

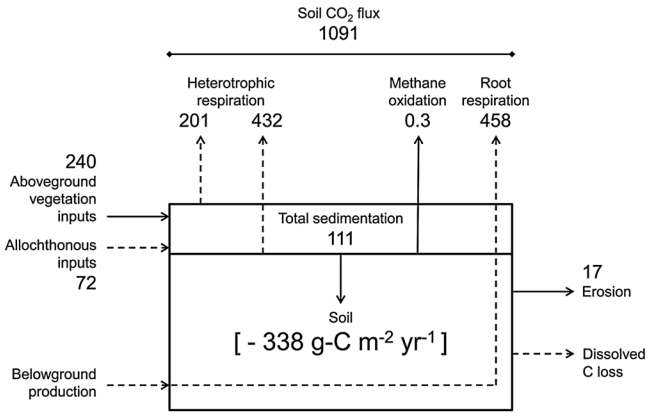

Figure 6. Average C budget for all sites. Values in g C m^{-2} yr^{-1}.

anaerobic processing. Conversely, larger grain sizes may promote aeration and methane oxidation. Surprisingly, CH_4 fluxes also did not vary significantly with sedimentation or vegetative fluxes of C or N; they also did not correlate with soil or sediment organic matter. Fluxes were negatively correlated with litter and sediment C:N and C:P, suggesting either substrate limitation by methanotrophs, nutrient limitation by methanogens, or covariation with hydrologic gradients. N_2O fluxes averaged zero, but showed some subtle pattern controls on anaerobic processes similar to CH_4. Specifically, N_2O flux was stimulated in wetter soils with greater sediment deposition rates.

4.4. C Budget

The Difficult Run C budget appears to be influenced greatly by both autochthonous and allochthonous C inputs, as well as aerobic respiration (Figure 6). Overall, these dry, short-hydroperiod floodplain wetlands were a net source of C to the atmosphere as CO_2 but were a very minor CH_4 sink of 0.3 g C m^{-2} yr^{-1} and did not contribute N_2O to the atmosphere. On average, the floodplain soils released 338 g C m^{-2} yr^{-1}, ranging from 259 to 529 g C m^{-2} yr^{-1}. Although oxidation of CH_4 released a small flux of 0.3 g of CO_2 C m^{-2} yr^{-1}, the radiative forcing equivalent of 7.5 g CO_2 C m^{-2} yr^{-1} (25:1 for CH_4:CO_2) [*Forster et al.*, 2007], methane oxidation is still a small proportion compared to total losses. Similar C fluxes of 232–463 g C m^{-2} yr^{-1} from GHGs alone were found along the Savannah River floodplain, of which CH_4 contributed $<$ 1% (or 1.6–4.0% based on radiative forcing [*Krauss and Whitbeck*, 2012]). Disturbed wetlands are estimated to release potentially 250–1000 g C m^{-2} yr^{-1} [*Mitra et al.*, 2005], and CO_2 is the primary component of gaseous C loss from wetlands [*Bridgham and Richardson*, 1992] as we also discovered for the Difficult Run watershed.

The 338 g C m^{-2} yr^{-1} loss is an estimated value, as we made several assumptions and omissions that could influence the final budget. Stored soil carbon is likely being lost through respiration faster than inputs of carbon from sedimentation or aboveground and belowground production. Even with the uncertainty in our C budget, these floodplains are likely a net source of C to the atmosphere. For example, root respiration is a major part of the budget, which we estimated as an average proportion of total soil CO_2 flux for temperate deciduous forests [*Subke et al.*, 2006]; however, these literature values ranged widely from 4 to 71%. Small changes in the fraction of root respiration would significantly alter the amount of CO_2 emissions due to heterotrophic soil respiration. Furthermore, total CO_2 fluxes may have been underestimated by up to 15% due to PVC collar insertion severing fine roots near the surface [*Heinemeyer et al.*, 2011]. However, our collars were inserted one month prior to the first sampling, and over 2 years of study, it is likely that many fine roots grew back. Root respiration is not included in the calculation of soil C loss, but heterotrophic respiration rates could also be calculated higher if overall CO_2 flux were underestimated.

We also did not measure belowground production but assumed it to be steady state for the duration of our sampling, in which sites are not actively changing. Belowground production was thus accounted for in the root respiration and heterotrophic flux. However, there would be some root C inputs to soil C storage, lowering the total amount of C lost. One budget of a deciduous forest floor measured 20% of CO_2 flux due to litter decay, 35% due to root respiration, 42% due to root decay, and the small remainder due to soil organic matter respiration [*Edwards and Harris*, 1977]. Our budget is similar: 18% of CO_2 flux due to litter decay, 42% due to root respiration, and the remaining 40% due to combined root decay and soil organic matter respiration.

We also did not measure dissolved inorganic carbon (DIC), dissolved organic carbon (DOC), or particulate organic carbon (POC) losses from the floodplain soil. Dissolved carbon is a large part of the C budget and

©2014. American Geophysical Union. All Rights Reserved.

important for microbial processing, and any autochthonous inputs that were lost or respired as dissolved CO_2 or DOC were not accounted for and could increase our estimate of C loss. In a Georgia floodplain, surface and groundwater exports of DIC were a small part of the budget, but DOC export was large [*Pulliam*, 1993]. However, the floodplain of Difficult Run is not a long-hydroperiod, blackwater system with large organic exports from the floodplain. In an Amazon headwater system, groundwater discharge of respired CO_2 was a large portion of the C budget and fate for terrestrially respired C [*Johnson et al*., 2008]. Yet in created riparian wetlands in Ohio, C inputs were mainly balanced with C sequestration and outflows; there did not appear to be any net loss of dissolved C or POC [*Waletzko and Mitsch*, 2013]. In our study, 5 of 105 feldspar marker horizons were net erosional, and by not directly measuring soil POC loss, we did slightly underestimate our total C loss.

One hypothesis for the net loss of C from the Difficult Run floodplain is that it has been drying due to urbanization of the watershed. Human alterations, such as watershed "hardening" due to the increase in impervious surface, can disconnect rivers from their floodplains and reduce flooding and sedimentation [*Groffman et al*., 2003; *Thoms*, 2003; *Hupp et al*., 2009]. Watershed imperviousness from development reduces groundwater recharge and incises stream channels, resulting in water table drawdown in floodplain soils [*Groffman et al*., 2003]. Impervious surfaces covered 18% of the Difficult Run watershed by 1997 [*Slonecker and Tilley*, 2004], following a land use shift from rural to mixed urban and suburban development starting in the mid-1960s. We found a weak negative trend in low-flow discharges (25th percentile) over the period of record of discharge at the mouth of the watershed (1935–2012; Figure 4), which spans the period of land use change. This decline in base flow is likely indicative of long-term lowering of the water table and drying of surficial soils in the floodplain. Floodplain drying is most likely attributable to watershed urbanization, but legacy sediment deposition and contemporary floodplain accretion, natural disturbances, or climatic changes in precipitation also could have been drying out the surface soils of the floodplain.

But urbanization also can potentially increase flooding and C inputs to floodplain soils. Difficult Run had an average flood return interval of 1.11 years prior to 1965, but rapid urbanization in the 1960s has made the system more flashy with a significantly increased flood frequency (0.23 years) [*Hupp et al*., 2013]. Increased flooding may deliver more allochthonous C to floodplain soils, potentially offsetting enhanced soil respiration in the C budget. However, the site with the greatest rate of allochthonous C trapping in the watershed still had a net loss of C from soils. Furthermore, C sedimentation can also stimulate soil and sediment respiration by providing electron donors that stimulate C turnover or nutrients that stimulate microbial respiration, though we did not find direct correlations between respiration rates and C inputs here. In summary, this floodplain became a source of atmospheric C driven by changes in hydrology that increased soil oxygenation, despite allochthonous C sedimentation; our C balance represented an annual loss of 1.7% of the floodplain C stock. In the long term, we expect the C budget will become balanced as soil respiration equilibrates to C inputs.

5. Conclusions

Surprisingly, inputs of C from sedimentation and vegetative litter production did not stimulate soil greenhouse gas efflux in a floodplain. Instead, CO_2 and CH_4 fluxes varied significantly along lateral and longitudinal gradients in hydrologic connectivity, soil wetness, and sediment texture. CO_2 fluxes increased at drier sites with coarser sediment (particularly levees) and CH_4 fluxes increased at wetter sites with finer texture (particularly backswamps). The results suggest that soil C respiration is determined more by soil wetness than C inputs and that much deposited C may not be labile to soil microbes. These relatively dry floodplain wetlands were not a significant source of the powerful greenhouse gases methane and nitrous oxide. On average, methane was consumed but the flux was a small proportion of the CO_2 flux. Carbon deposition exceeded bank erosion at all sites, suggesting that these floodplains are a fluvial sink of particulate C. The overall C budget was dominated by soil CO_2 flux and not balanced, with outputs exceeding inputs, making these floodplain wetland soils a net C source. Floodplain drying associated with urbanization has likely caused a short-term net release of CO_2-C as microbial respiration depletes long-term storage of soil C, but we predict that these floodplain wetlands will become carbon neutral (neither a net storage nor sink) in the long term as fluxes match inputs after disturbance.

©2014. American Geophysical Union. All Rights Reserved.

Acknowledgments
Data from this study are available from Gregory B. Noe upon request. Support for this project was provided by the USGS National Research Program, USGS Chesapeake Priority Ecosystem Science Program, USGS Hydrologic Networks and Analyses Program, and USGS Climate and Land Use Change Research and Development Program. We thank Rebecca F. Moss for conducting laboratory analyses on the GC; Krystal Bealing, Sarah Ulrich, Andrew Kunz, Sydney Salley, Adam Benthem, Alice Besterman, and Scott Ensign for assistance in the field; and the reviewers of the manuscript. Any use of trade, product, or firm names is for descriptive purposes only and does not imply endorsement by the U.S. Government.

References

Altor, A. E., and W. J. Mitsch (2006), Methane flux from created riparian marshes: Relationship to intermittent versus continuous inundation and emergent macrophytes, *Ecol. Eng.*, *28*, 224–234, doi:10.1016/j.ecoleng.2006.06.006.

Altor, A. E., and W. J. Mitsch (2008), Methane and carbon dioxide dynamics in wetland mesocosms: Effects of hydrology and soils, *Ecol. Appl.*, *18*, 1307–1320, doi:10.1890/07-0009.1.

Amoros, C., A. L. Roux, J. L. Reygrobellet, J. P. Bravard, and G. Pautou (1987), A method for applied ecological studies of fluvial hydrosystems, *Reg. Rivers Res. Manage.*, *1*(1), 17–36, doi:10.1002/rrr.3450010104.

Bartlett, K. B., P. M. Crill, J. A. Bonassi, J. E. Richey, and R. C. Harriss (1990), Methane flux from the Amazon River floodplain: Emissions during rising water, *J. Geophys. Res. (1984–2012)*, *95*(D10), 16,773–16,788, doi:10.1029/JD095iD10p16773.

Battin, T. J., L. A. Kaplan, S. Findlay, C. S. Hopkinson, E. Marti, A. I. Packman, J. D. Newbold, and F. Sabater (2008), Biophysical controls on organic carbon fluxes in fluvial networks, *Nat. Geosci.*, *1*, 95–100, doi:10.1038/ngeo101.

Battin, T. J., S. Luyssaert, L. A. Kaplan, A. K. Aufdenkampe, A. Richter, and L. J. Tranvik (2009), The boundless carbon cycle, *Nat. Geosci.*, *2*, 598–600, doi:10.1038/ngeo618.

Bayley, P. B. (1995), Understanding large river: Floodplain ecosystems, *BioScience*, *45*(3), 153–158, doi:10.2307/1312554.

Bond-Lamberty, B., and A. Thomson (2010), A global database of soil respiration data, *Biogeosciences*, *7*, 1915–1926.

Boon, P. I., and K. Lee (1997), Methane oxidation in sediments of a floodplain wetland in south-eastern Australia, *Lett. Appl. Microbiol.*, *25*(2), 138–142, doi:10.1046/j.1472-765X.1997.00189.x.

Boon, P. I., A. Mitchell, and K. Lee (1997), Effects of wetting and drying on methane emissions from ephemeral floodplain wetlands in south-eastern Australia, *Hydrobiologia*, *357*(1–3), 73–87, doi:10.1023/A:1003126601466.

Bridgham, S. D., and C. J. Richardson (1992), Mechanisms controlling soil respiration (CO2 and CH4) in southern peatlands, *Soil Biol. Biochem.*, *24*(11), 1089–1099, doi:10.1016/0038-0717(92)90058-6.

Bridgham, S. D., K. Updegraff, and J. Pastor (1998), Carbon, nitrogen, and phosphorus mineralization in northern wetlands, *Ecology*, *79*(5), 1545–1561, doi:10.1890/0012-9658(1998)079[1545:CNAPMI]2.0.CO;2.

Bridgham, S. D., J. P. Megonigal, J. K. Keller, N. B. Bliss, and C. Trettin (2006), The carbon balance of North American wetlands, *Wetlands*, *26*, 889–916, doi:10.1672/0277-5212(2006)26[889:TCBONA]2.0.CO;2.

Brinson, M. M., A. E. Lugo, and S. Brown (1981), Primary productivity, decomposition and consumer activity in freshwater wetlands, *Annu. Rev. Ecol. Syst.*, *12*(1), 123–161, doi:10.1146/annurev.es.12.110181.001011.

Burke, M. K., B. G. Lockaby, and W. H. Conner (1999), Aboveground production and nutrient circulation along a flooding gradient in a South Carolina Coastal Plain forest, *Can. J. For. Res.*, *29*(9), 1402–1418, doi:10.1139/x99-111.

Casper, P., S. C. Maberly, G. H. Hall, and B. J. Finlay (2000), Fluxes of methane and carbon dioxide from a small productive lake to the atmosphere, *Biogeochemistry*, *49*(1), 1–19, doi:10.1023/A:1006269900174.

Clawson, R. G., B. G. Lockaby, and B. Rummer (2001), Changes in production and nutrient cycling across a wetness gradient within a floodplain forest, *Ecosystems*, *4*(2), 126–138, doi:10.1007/s100210000063.

Couwenberg, J., R. Dommain, and H. Joosten (2010), Greenhouse gas fluxes from tropical peatlands in south-east Asia, *Global Change Biol.*, *16*, 1715–1732, doi:10.1111/j.1365-2486.2009.02016.x.

Craft, C. B., and W. P. Casey (2000), Sediment and nutrient accumulation in floodplain and depressional freshwater wetlands of Georgia, USA, *Wetlands*, *20*(2), 323–332, doi:10.1672/0277-5212(2000)020[0323:SANAIF]2.0.CO;2.

Crill, P. M. (1991), Seasonal patterns of methane uptake and carbon dioxide release by a temperate woodland soil, *Global Biogeochem. Cycles*, *5*(4), 319–334, doi:10.1029/91GB02466.

Davidson, E. A., M. Keller, H. E. Erickson, L. V. Verchot, and E. Veldkamp (2000), Testing a conceptual model of soil emissions of nitrous and nitric oxides: Using two functions based on soil nitrogen availability and soil water content, the hole-in-the-pipe model characterizes a large fraction of the observed variation of nitric oxide and nitrous oxide emissions from soils, *BioScience*, *50*(8), 667–680, doi:10.1641/0006-3568(2000)050[0667:TACMOS]2.0.C.

DeBusk, W. F., and K. R. Reddy (2003), Nutrient and hydrology effects on soil respiration in a northern Everglades marsh, *J. Environ. Qual.*, *32*(2), 702–710, doi:10.2134/jeq2003.7020.

Edwards, N. T., and W. F. Harris (1977), Carbon cycling in a mixed deciduous forest floor, *Ecology*, *58*(2), 431–437.

Forster, P., et al. (2007), Changes in atmospheric constituents and in radiative forcing, in *Climate Change 2007: The Physical Science Basis. Contribution of Working Group I to the Fourth Assessment Report of the Intergovernmental Panel on Climate Change*, edited by S. Solomon et al., Cambridge Univ. Press, Cambridge, and New York.

Freeman, C., M. A. Lock, S. Hughes, B. Reynolds, and J. A. Hudson (1997), Nitrous oxide emissions and the use of wetlands for water quality amelioration, *Environ. Sci. Technol.*, *31*(8), 2438–2440, doi:10.1021/es9604673.

Fromin, N., G. Pinay, B. Montuelle, D. Landais, J. M. Ourcival, R. Joffre, and R. Lensi (2010), Impact of seasonal sediment desiccation and rewetting on microbial processes involved in greenhouse gas emissions, *Ecohydrology*, *3*, 339–348, doi:10.1002/eco.115.

Gallardo, B., C. Español, and F. A. Comin (2012), Aquatic metabolism short-term response to the flood pulse in a Mediterranean floodplain, *Hydrobiologia*, *693*, 251–264, doi:10.1007/s10750-012-1126-9.

Giblin, A. E., K. J. Nadelhoffer, G. R. Shaver, J. A. Laundre, and A. J. McKerrow (1991), Biogeochemical diversity along a riverside toposequence in arctic Alaska, *Ecol. Monogr.*, *61*(4), 415–435, doi:10.2307/2937049.

Gleason, R. A., B. A. Tangen, B. A. Browne, and N. H. Euliss Jr. (2009), Greenhouse gas flux from cropland and restored wetlands in the Prairie Pothole Region, *Soil Biol. Biochem.*, *41*, 2501–2507, doi:10.1016/j.soilbio.2009.09.008.

Goulden, M. L., S. D. Miller, H. R. Da Rocha, M. C. Menton, H. C. de Freitas, A. M. E. Silva Figueira, and C. A. D. de Sousa (2004), Diel and seasonal patterns of tropical forest CO2 exchange, *Ecol. Appl.*, *14*, 42–54, doi:10.1890/02-6008.

Groffman, P. M., and J. M. Tiedje (1991), Relationships between denitrification, CO2 production and air-filled porosity in soils of different texture and drainage, *Soil Biol. Biochem.*, *23*(3), 299–302, doi:10.1016/0038-0717(91)90067-T.

Groffman, P. M., D. J. Bain, L. E. Band, K. T. Belt, G. S. Brush, J. M. Grove, R. V. Pouyat, I. C. Yesilonis, and W. C. Zipperer (2003), Down by the riverside: Urban riparian ecology, *Front. Ecol. Environ.*, *1*(6), 315–321, doi:10.1890/1540-9295(2003)001[0315:DBTRUR]2.0.CO;2.

Groffman, P. M., J. P. Hardy, M. C. Fisk, T. J. Fahey, and C. T. Driscoll (2009), Climate variation and soil carbon and nitrogen cycling processes in a northern hardwood forest, *Ecosystems*, *12*, 927–943, doi:10.1007/s10021-009-9268-y.

Gulledge, J., and J. P. Schimel (2000), Controls on soil carbon dioxide and methane fluxes in a variety of taiga forest stands in interior Alaska, *Ecosystems*, *3*(3), 269–282, doi:10.1007/s100210000025.

Gupta, S. R., and J. S. Singh (1981), Soil respiration in a tropical grassland, *Soil Biol. Biochem.*, *13*(4), 261–268, doi:10.1016/0038-0717(81)90060-2.

Harriss, R. C., D. I. Sebacher, and F. P. Day (1982), Methane flux in the great dismal swamp, *Nature*, *297*(5868), 673–674, doi:10.1038/297673a0.

©2014. American Geophysical Union. All Rights Reserved.

Healy, R. W., R. G. Striegl, T. F. Russell, G. L. Hutchinson, and G. P. Livingston (1996), Numerical evaluation of static-chamber measurements of soil-atmosphere gas exchange: Identification of physical processes, *Soil Sci. Soc. Am. J.*, *60*(3), 740–747, doi:10.2136/sssaj1996.03615995006000030009x.

Hedges, J. I., and J. H. Stern (1984), Carbon and nitrogen determinations of carbonate-containing solids, *Limnol. Oceanogr.*, *29*(3), 657–663.

Heinemeyer, A., C. Di Bene, A. R. Lloyd, D. Tortorella, R. Baxter, B. Huntley, A. Gelsomino, and P. Ineson (2011), Soil respiration: Implications of the plant-soil continuum and respiration chamber collar-insertion depth on measurement and modelling of soil CO2 efflux rates in three ecosystems, *Eur. J. Soil Sci.*, *62*, 82–94, doi:10.1111/j.1365-2389.2010.01331.x.

Hopkinson, C. S. (1992), A comparison of ecosystem dynamics in freshwater wetlands, *Estuaries*, *15*(4), 549–562, doi:10.2307/1352397.

Hupp, C. R. (1986), The headward extent of fluvial landforms and associated vegetation on Massanutten Mountain, Virginia, *Earth Surf. Processes Landforms*, *11*(5), 545–555, doi:10.1002/esp.3290110509.

Hupp, C. R. (2000), Hydrology, geomorphology and vegetation of Coastal Plain rivers in the south-eastern USA, *Hydrol. Processes*, *14*(16-17), 2991–3010.

Hupp, C. R., C. R. Demas, D. E. Kroes, R. H. Day, and T. W. Doyle (2008), Recent sedimentation patterns within the central Atchafalaya Basin, Louisiana, *Wetlands*, *28*, 125–140, doi:10.1672/06-132.1.

Hupp, C. R., A. R. Pierce, and G. B. Noe (2009), Floodplain geomorphic processes and environmental impacts of human alteration along coastal plain rivers, USA, *Wetlands*, *29*, 413–429, doi:10.1672/08-169.1.

Hupp, C. R., G. B. Noe, E. R. Schenk, and A. J. Bentham (2013), Recent and historic sediment dynamics along Difficult Run, a suburban Virginia Piedmont stream, *Geomorphology*, *180–181*, 156–169, doi:10.1016/j.geomorph.2012.10.007.

Jaatinen, K., R. Laiho, A. Vuorenmaa, U. Del Castillo, K. Minkkinen, T. Pennanen, T. Penttilä, and H. Fritze (2008), Responses of aerobic microbial communities and soil respiration to water-level drawdown in a northern boreal fen, *Environ. Microbiol.*, *10*, 339–353, doi:10.1111/j.1462-2920.2007.01455.x.

Johnson, M. S., J. Lehmann, S. J. Riha, A. V. Krusche, J. E. Richey, J. P. H. B. Ometto, and E. G. Couto (2008), CO2 efflux from Amazonian headwater streams represents a significant fate for deep soil respiration, *Geophys. Res. Lett.*, *35*, *L17401*, doi:10.1029/2008GL034619.

Jolley, R. L., B. G. Lockaby, and R. M. Governo (2010), Biogeochemical influences associated with sedimentation in riparian forests of the Southeastern Coastal Plain, *Soil Sci. Soc. Am. J.*, *74*, 326–336, doi:10.2136/sssaj2009.0041.

Junk, W. J., P. B. Bayley, and R. E. Sparks (1989), The flood pulse concept in river-floodplain systems, *Can. Spec. Publ. Fish. Aquat. Sci.*, *106*(1), 110–127.

Koh, H.-S., C. A. Ochs, and K. Yu (2009), Hydrologic gradient and vegetation controls on CH4 and CO2 fluxes in a spring-fed forested wetland, *Hydrobiologia*, *630*, 271–286, doi:10.1007/s10750-009-9821-x.

Krauss, K. W., and J. L. Whitbeck (2012), Soil greenhouse gas fluxes during wetland forest retreat along the lower Savannah River, Georgia (USA), *Wetlands*, *32*, 73–81, doi:10.1007/s13157-011-0246-8.

Krauss, K. W., J. L. Whitbeck, and R. J. Howard (2012), On the relative roles of hydrology, salinity, temperature, and root productivity in controlling soil respiration from coastal swamps (freshwater), *Plant Soil*, *358*, 265–274, doi:10.1007/s11104-012-1182-y.

Le Mer, J., and P. Roger (2001), Production, oxidation, emission and consumption of methane by soils: A review, *Eur. J. Soil Biol.*, *37*(1), 25–50, doi:10.1016/S1164-5563(01)01067-6.

Lockaby, B. G., and M. R. Walbridge (1998), Biogeochemistry, in *Southern Forested Wetlands: Ecology and Management*, edited by M. G. Messina and W. H. Conner, pp. 149–172, CRC Press, Boca Raton, Fla.

McClain, M. E., E. W. Boyer, C. L. Dent, S. E. Gergel, N. B. Grimm, P. M. Groffman, S. C. Hart, J. W. Harvey, C. A. Johnston, and E. Mayorga (2003), Biogeochemical hot spots and hot moments at the interface of terrestrial and aquatic ecosystems, *Ecosystems*, *6*(4), 301–312, doi:10.1007/s10021-003-0161-9.

Megonigal, J. P., and W. H. Schlesinger (1997), Enhanced CH4 emission from a wetland soil exposed to elevated CO2, *Biogeochemistry*, *37*(1), 77–88, doi:10.1023/A:1005738102545.

Miao, G., A. Noormets, J. C. Domec, C. C. Trettin, S. G. McNulty, G. Sun, and J. S. King (2013), The effect of water table fluctuation on soil respiration in a lower coastal plain forested wetland in the southeastern US, *J. Geophys. Res. Biogeosci.*, *118*, 1–15, doi:10.1002/2013JG002354.

Mitra, S., R. Wassmann, and P. L. G. Vlek (2005), An appraisal of global wetland area and its organic carbon stock, *Curr. Sci.*, *88*, 25.

Mitsch, W. J., and J. G. Gosselink (2007), *Wetlands*, John Wiley, Hoboken, N. J.

Moore, T. R., and M. Dalva (1997), Methane and carbon dioxide exchange potentials of peat soils in aerobic and anaerobic laboratory incubations, *Soil Biol. Biochem.*, *29*(8), 1157–1164, doi:10.1016/S0038-0717(97)00037-0.

Moore, T. R., and R. Knowles (1989), The influence of water table levels on methane and carbon dioxide emissions from peatland soils, *Can. J. Soil Sci.*, *69*(1), 33–38, doi:10.4141/cjss89-004.

Moosavi, S. C., and P. M. Crill (1997), Controls on CH4 and CO2 emissions along two moisture gradients in the Canadian boreal zone, *J Geophys Res (1984–2012)*, *102*(D24), 29,261–29,277, doi:10.1029/96JD03873.

Morse, J. L., M. Ardón, and E. S. Bernhardt (2012), Greenhouse gas fluxes in southeastern US coastal plain wetlands under contrasting land uses, *Ecol. Appl.*, *22*, 264–280, doi:10.1890/11-0527.1.

Nahlik, A. M., and W. J. Mitsch (2010), Methane emissions from created riverine wetlands, *Wetlands*, *30*, 783–793, doi:10.1007/s13157-010-0038-6.

Naiman, R. J., and H. Décamps (1997), The ecology of interfaces: Riparian zones, *Annu. Rev. Ecol. Syst.*, *28*(1), 621–658, doi:10.1146/annurev.ecolsys.28.1.621.

Nelson, D. W., and L. E. Sommers (1996), Total carbon, organic carbon and organic matter, in *Methods of Soil Analysis. Part 3: Chemical Methods*, edited by D. L. Sparks, pp. 961–1010, Soil Science Society of America, Madison, Wis.

Noe, G. B. (2011), Measurement of net nitrogen and phosphorus mineralization in wetland soils using a modification of the resin-core technique, *Soil Sci. Soc. Am. J.*, *75*, 760–770, doi:10.2136/sssaj2010.0289.

Noe, G. B. (2013), Interactions among hydrogeomorphology, vegetation, and nutrient biochemistry in floodplain ecosystems, in *Treatise on Geomorphology*, edited by J. Shroder et al., pp. 307–321, Academic Press, San Diego, Calif.

Noe, G. B., and C. R. Hupp (2005), Carbon, nitrogen, and phosphorus accumulation in floodplains of Atlantic Coastal Plain rivers, USA, *Ecol. Appl.*, *15*, 1178–1190, doi:10.1890/04-1677.

Noe, G. B., and C. R. Hupp (2009), Retention of riverine sediment and nutrient loads by coastal plain floodplains, *Ecosystems*, *12*, 728–746, doi:10.1007/s10021-009-9253-5.

Noe, G. B., C. R. Hupp, and N. B. Rybicki (2013), Hydrogeomorphology influences soil nitrogen and phosphorus mineralization in floodplain wetlands, *Ecosystems*, *16*, 75–94, doi:10.1007/s10021-012-9597-0.

©2014. American Geophysical Union. All Rights Reserved.

Poole, G. C. (2010), Stream hydrogeomorphology as a physical science basis for advances in stream ecology, *J. North Am. Benthol. Soc.*, *29*, 12–25, doi:10.1899/08-070.1.

Pulliam, W. M. (1993), Carbon dioxide and methane exports from a southeastern floodplain swamp, *Ecol. Monogr.*, *63*(1), 29–53, doi:10.2307/2937122.

Reddy, K. R., and R. D. DeLaune (2008), *Biogeochemistry of Wetlands: Science and Applications*, CRC Press, Boca Raton, Fla.

Richardson, W. B., E. A. Strauss, L. A. Bartsch, E. M. Monroe, J. C. Cavanaugh, L. Vingum, and D. M. Soballe (2004), Denitrification in the Upper Mississippi River: Rates, controls, and contribution to nitrate flux, *Can. J. Fish. Aquat. Sci.*, *61*, 1102–1112, doi:10.1139/f04-062.

Richey, J. E., A. H. Devol, S. C. Wofsy, R. Victoria, and M. N. G. Riberio (1988), Biogenic gases and the oxidation and reduction of carbon in Amazon River and floodplain waters, *Limnol. Oceanogr.*, *33*(1), 551–561, doi:10.4319/lo.1988.33.4.0551.

Robertson, G. P., P. Sollins, B. G. Ellis, and K. Lajtha (1999), Exchangeable ions, pH, and cation exchange capacity, in *Standard Soil Methods for Long-Term Ecological Research*, edited by G. P. Robertson et al., pp. 106–114, Oxford Univ. Press, New York.

Samaritani, E., J. Shrestha, B. Fournier, E. Frossard, F. Gillet, C. Guenat, P. A. Niklaus, N. Pasquale, K. Tockner, and E. A. D. Mitchell (2013), Heterogeneity of soil carbon pools and fluxes in a channelized and a restored floodplain section (Thur River, Switzerland), *Hydrol. Earth Syst. Sci.*, *15*, 1757–1769, doi:10.5194/hess-15-1757-2011.

Sánchez-Andrés, R., S. Sánchez-Carrillo, M. J. Ortiz-Llorente, M. Álvarez-Cobelas, and S. Cirujano (2010), Do changes in flood pulse duration disturb soil carbon dioxide emissions in semi-arid floodplains?, *Biogeochemistry*, *101*, 257–267, doi:10.1007/s10533-010-9472-z.

Schenk, E. R., C. R. Hupp, A. Gellis, and G. Noe (2012), Developing a new stream metric for comparing stream function using a bank-floodplain sediment budget: A case study of three Piedmont streams, *Earth Surf. Processes Landforms*, *38*, 771–784, doi:10.1002/esp.3314.

Segers, R. (1998), Methane production and methane consumption: A review of processes underlying wetland methane fluxes, *Biogeochemistry*, *41*(1), 23–51, doi:10.1023/A:1005929032764.

Sha, C., W. J. Mitsch, Ü. Mander, J. Lu, J. Batson, L. Zhang, and W. He (2011), Methane emissions from freshwater riverine wetlands, *Ecol. Eng.*, *37*, 16–24, doi:10.1016/j.ecoleng.2010.07.022.

Sjögersten, S., R. van der Wal, and S. J. Woodin (2006), Small-scale hydrological variation determines landscape CO2 fluxes in the high Arctic, *Biogeochemistry*, *80*, 205–216, doi:10.1007/s10533-006-9018-6.

Slonecker, E. T., and J. S. Tilley (2004), An evaluation of the individual components and accuracies associated with the determination of impervious area, *Glsci. Remote Sens.*, *41*, 165–184.

Smith, L. K., W. M. Lewis Jr., J. P. Chanton, G. Cronin, and S. K. Hamilton (2000), Methane emissions from the Orinoco River floodplain, Venezuela, *Biogeochemistry*, *51*(2), 113–140, doi:10.1023/A:1006443429909.

Spink, A., R. E. Sparks, M. Van Oorschot, and J. T. A. Verhoeven (1998), Nutrient dynamics of large river floodplains, *Reg. Rivers Res. Manage.*, *14*(2), 203–216, doi:10.1002/(SICI)1099-1646(199803/04)14:2<203:AID-RRR498>3.0.CO;2-7.

Subke, J.-A., I. Inglima, and M. Francesca Cotrufo (2006), Trends and methodological impacts in soil CO2 efflux partitioning: A metaanalytical review, *Global Change Biol.*, *12*, 921–943, doi:10.1111/j.1365-2486.2006.01117.x.

Terazawa, K., S. Ishizuka, T. Sakata, K. Yamada, and M. Takahashi (2007), Methane emissions from stems of Fraxinus mandshurica var. japonica trees in a floodplain forest, *Soil Biol. Biochem.*, *39*, 2689–2692, doi:10.1016/j.soilbio.2007.05.013.

Thoms, M. C. (2003), Floodplain-river ecosystems: Lateral connections and the implications of human interference, *Geomorphology*, *56*(3), 335–349, doi:10.1016/S0169-555X(03)00160-0.

Tockner, K., and J. A. Stanford (2002), Riverine flood plains: Present state and future trends, *Environ. Conserv.*, *29*(03), 308–330, doi:10.1017/S037689290200022X.

Updegraff, K., J. Pastor, S. D. Bridgham, and C. A. Johnston (1995), Environmental and substrate controls over carbon and nitrogen mineralization in northern wetlands, *Ecol. Appl.*, *5*(1), 151–163, doi:10.2307/1942060.

Updegraff, K., S. D. Bridgham, J. Pastor, P. Weishampel, and C. Harth (2001), Response of CO2 and CH4 emissions from peatlands to warming and water table manipulation, *Ecol. Appl.*, *11*(2), 311–326, doi:10.1890/1051-0761(2001)011[0311:ROCACE]2.0.CO;2.

US Geological Survey (2013), *Water Data Report 2013–01646000 Difficult Run near Great Falls, VA*, US Geological Survey, Reston, Va.

Valett, H. M., M. A. Baker, J. A. Morrice, C. S. Crawford, M. C. Molles Jr., C. N. Dahm, D. L. Moyer, J. R. Thibault, and L. M. Ellis (2005), Biogeochemical and metabolic responses to the flood pulse in a semiarid floodplain, *Ecology*, *86*, 220–234, doi:10.1890/03-4091.

Vannote, R. L., G. W. Minshall, K. W. Cummins, J. R. Sedell, and C. E. Cushing (1980), The river continuum concept, *Can. J. Fish. Aquat. Sci.*, *37*(1), 130–137, doi:10.1139/f80-017.

Verhoeven, J. T. A., B. Arheimer, C. Yin, and M. M. Hefting (2006), Regional and global concerns over wetlands and water quality, *Trends Ecol. Evol.*, *21*, 96–103, doi:10.1016/j.tree.2005.11.015.

Waletzko, E. J., and W. J. Mitsch (2013), The carbon balance of two riverine wetlands fifteen years after their creation, *Wetlands*, *33*, 989–999, doi:10.1007/s13157-013-0457-2.

Ward, J. V. (1989), River-wetland interactions, in *Freshwater Wetlands and Wildlife*, edited by R. R. Sharitz and J. W. Gibbons, pp. 385–400, USDOE Office of Scientific and Technical Information, Oak Ridge, Tenn.

Welti, N., E. Bondar-Kunze, G. Singer, M. Tritthart, S. Zechmeister-Boltenstern, T. Hein, and G. Pinay (2012), Large-scale controls on potential respiration and denitrification in riverine floodplains, *Ecol. Eng.*, *42*, 73–84, doi:10.1016/j.ecoleng.2012.02.005.

Whiting, G. J., and J. P. Chanton (1993), Primary production control of methane emission from wetlands, *Nature*, *364*(6440), 794–795, doi:10.1038/364794a0.

Whiting, G. J., J. P. Chanton, D. S. Bartlett, and J. D. Happell (1991), Relationships between CH4 emission, biomass, and CO2 exchange in a subtropical grassland, *J. Geophys. Res. (1984–2012)*, *96*(D7), 13,067–13,071, doi:10.1029/91JD01248.

Wickland, K. P., R. G. Striegl, S. K. Schmidt, and M. A. Mast (1999), Methane flux in subalpine wetland and unsaturated soils in the southern Rocky Mountains, *Global Biogeochem. Cycles*, *13*(1), 101–113, doi:10.1029/1998GB900003.

Wickland, K. P., J. C. Neff, and J. W. Harden (2010), The role of soil drainage class in carbon dioxide exchange and decomposition in boreal black spruce (*Picea mariana*) forest stands, *Can. J. For. Res.*, *40*, 2123–2134, doi:10.1139/X10-163.

Wilson, J. S., D. S. Baldwin, G. N. Rees, and B. P. Wilson (2011), The effects of short-term inundation on carbon dynamics, microbial community structure and microbial activity in floodplain soil, *River Res. Appl.*, *27*, 213–225, doi:10.1002/rra.1352.

Wolf, K. L., G. B. Noe, and C. Ahn (2013), Hydrologic connectivity to streams increases nitrogen and phosphorus inputs and cycling in soils of created and natural floodplain wetlands, *J. Environ. Qual.*, *42*, 1245–1255, doi:10.2134/jeq2012.0466.

Yu, K., S. P. Faulkner, and M. J. Baldwin (2008), Effect of hydrological conditions on nitrous oxide, methane, and carbon dioxide dynamics in a bottomland hardwood forest and its implication for soil carbon sequestration, *Global Change Biol.*, *14*, 798–812, doi:10.1111/j.1365-2486.2008.01545.x.

Zehetner, F., G. J. Lair, and M. H. Gerzabek (2009), Rapid carbon accretion and organic matter pool stabilization in riverine floodplain soils, *Global Biogeochem. Cycles*, *23*, GB4004, doi:10.1029/2009GB003481.

©2014. American Geophysical Union. All Rights Reserved.